Lax Entropy Conditions for the One-Dimensional Riemann Problem

THESIS

submitted in partial fulfillment of the
requirements for the degree of

BACHELOR OF SCIENCE
in
PHYSICS AND ASTRONOMY

Author :	Johannes Post
Student ID :	s2033429
Supervisor :	Prof. Dr. Koenraad Schalm
	Dr. Christian Ecker
2^{nd} corrector :	Prof. Dr. Vincent Icke

Leiden, The Netherlands, June 19, 2020

Lax Entropy Conditions for the One-Dimensional Riemann Problem

Johannes Post

Institute Lorentz for Theoretical Physics, Leiden University
P.O. Box 9500, 2300 RA Leiden, The Netherlands

June 19, 2020

Abstract

To find solutions to systems of conservation laws with discontinuities, weak solutions will be studied. To pick a unique weak solution one requires some additional conditions. In this thesis we will see that for the Riemann problem in one spatial dimension, the Lax entropy conditions are a way to do this. By considering the Euler equations we will see that these conditions are equivalent to the second law of thermodynamics and therefore pick the physically relevant solution. Furthermore, we construct numerical solutions to a specific Riemann problem using a standard discretization method and a method based on nonlinear shocks, followed by a on discussion their strengths and weaknesses.

Contents

Chapter 1

Introduction

Conservation laws are at the basis of physics. Local conservation laws describe physical phenomena relating the time variation of a quantity to the transport of this quantity. Conservation laws consist of partial differential equations which can be mathematically analysed. The goal is to find an expression explaining the evolution of the conserved quantity. In certain cases however, most notably for large deviations outside the linear regime, these formal solutions can develop discontinuities after some finite time. At that moment, these solutions will break down. This is because our conservation laws consist of partial differential equations (PDE's) and derivatives of discontinuous functions are not defined.

A prominent example of a conservation law is charge conservation, which can be derived from the Maxwell equations. This conservation law is given by the continuity equation for the charge density:

$$\nabla \cdot \mathbf{J} = -\frac{\partial \rho}{\partial t}, \tag{1.1}$$

where ρ is the charge density, $\mathbf{J}$ is the current density. This equation can equivalently be written as

$$\frac{\partial \rho}{\partial t} + \sum_{j=1}^{3} \frac{\partial J_j}{\partial x_j} = 0. \tag{1.2}$$

A specific problem is the Riemann problem. The Riemann problem is an initial value problem containing a jump discontinuity in the initial data. For example if two regions of constant temperature are joined together, the jump in temperature is a discontinuity. By studying the Riemann problem, the propagation of discontinuities can be better understood. As will be seen in Chapter 3, initial value problems for conservation laws also can develop discontinuities, even when the initial data is smooth. The knowledge on the propagation of discontinuities can therefore be applied to all systems of conservation laws, as discontinuities might develop over time.

To find a description of the conserved quantity, while being discontinuous, we must look at a larger class of solutions called *weak solutions*. When we think of the Heaviside step function, we know that we cannot differentiate this function in the point where the step is taken. However when we integrate the differential equations together with another function (called the 'test function'), we can show that our solution does not need to be differentiable in every point to satisfy this integrated conservation law. This larger class of solutions, called weak solutions, allows for certain discontinuities to exist.

However, allowing for this larger class of solutions comes at the cost of non-uniqueness. It can be shown that in general the solution is not unique, and in many cases there is an infinite number of solutions. Then an additional condition is necessary to pick a unique solution. Furthermore one wishes that this unique solution

will also be the physical correct one. A way that this is done, is by generalising the thermodynamic notion of entropy and enforcing entropy conditions on our system, just like the second law of thermodynamics does. Specifically for the Riemann problem in one spatial dimension, Lax[1, 2] introduced entropy conditions on the allowed propagation speeds of the discontinuities (the shock waves). However, most literature concerning these entropy conditions is rather mathematical and does not always explain how this mathematically defined condition relates to the physical notion of entropy. One goal of this work is to explore the Riemann problem and the entropy conditions to understand them both mathematically and physically and to find whether these conditions indeed pick the physical correct solution.

We will start in Chapter 2 by mathematically describing conservation laws and introduce the Riemann problem. In Chapter 3 we show that there is in general not a solution to this problem beyond some finite time and therefore introduce a broader class of solutions. Then we derive that these solution should satisfy certain conditions around the discontinuities and we show that this type of solution in not unique. We then explore this non-uniqueness numerically. In Chapter 4 we introduce the general mathematical notion of entropy that can be used to select a unique solution. Then in Chapter 5 we explain the specific entropy conditions for the Riemann problem in one dimension and how these conditions relate to the second law of thermodynamics. In Chapter 6 we present numerical solutions to a specific Riemann problem with self written codes implementing Roe-averaging, which inherently builds on the propagation of discontinuities and weak solutions, and two discretization methods: the Forward-Time Central-Space method and the Lax-Friedrichs method, of which the latter one always smoothens out the discontinuities such that they formally do not exist. The thesis in concluded with a discussion in a Chapter 7.

Chapter 2

Mathematical Framework and Definitions

To start we need to review the mathematical framework of conservation laws and the Riemann problem. The discussion and notation in this chapter and next chapter will closely follow the textbook by Godlewski and Raviart [3].

We begin by stating the general form of conservation laws in multiple variables:

$$\frac{\partial \mathbf{u}}{\partial t} + \sum_{j=1}^{d} \frac{\partial}{\partial x_j} \mathbf{f}_j(\mathbf{u}) = \mathbf{0}, \qquad \mathbf{x} = (x_1, \ldots, x_d) \in \mathbb{R}^d, t > 0, \tag{2.1}$$

where $\mathbf{u}$ is the vector of conserved quantities and $\mathbf{f}_j$ are the flux vectors associated with these conserved quantities. Furthermore $\mathbf{u} = \mathbf{u}(\mathbf{x}, t)$ is a function of space and time.

An example can be given by the Euler equations of compressible fluid flow

$$\frac{\partial \rho}{\partial t} + \nabla \cdot \rho \mathbf{v} = 0, \tag{2.2}$$

$$\frac{\partial \rho \mathbf{v}}{\partial t} + \nabla \cdot (\rho \mathbf{v} \otimes \mathbf{v} + p\mathbf{I}) = 0, \tag{2.3}$$

$$\frac{\partial \rho e}{\partial t} + \nabla \cdot ((\rho e + p)\mathbf{v}) = 0. \tag{2.4}$$

Where ρ is the mass density, $\mathbf{v}$ is the velocity flow vector field, p is the pressure, $e = \varepsilon + \frac{u^2}{2}$ is the total specific energy and ε is the internal specific energy. Here ρ, $\mathbf{v}$ and e are all functions of $\mathbf{x}$ and t. The first of these equations represents mass conservation, the second momentum conservation and the third energy conservation. These can be put in the form of (2.1) by setting

$$\mathbf{u} = \begin{pmatrix} \rho \\ \rho v_1 \\ \rho v_2 \\ \rho v_3 \\ \rho e \end{pmatrix}, \quad \mathbf{f}_1(\mathbf{u}) = \begin{pmatrix} \rho v_1 \\ \rho v_1^2 + p \\ \rho v_1 v_2 \\ \rho v_1 v_3 \\ (\rho e + p) v_1 \end{pmatrix}, \quad \mathbf{f}_2(\mathbf{u}) = \begin{pmatrix} \rho v_2 \\ \rho v_2 v_1 \\ \rho v_2^2 + p \\ \rho v_2 v_3 \\ (\rho e + p) v_2 \end{pmatrix}, \quad \mathbf{f}_3(\mathbf{u}) = \begin{pmatrix} \rho v_3 \\ \rho v_3 v_1 \\ \rho v_3 v_2 \\ \rho v_3^2 + p \\ (\rho e + p) v_3 \end{pmatrix}. \tag{2.5}$$

Conservation laws can also be written in a more intuitive form. Let D be an arbitrary domain in space, and let $\mathbf{n} = (n_1, \ldots, n_d)$ be the outward unit normal to the boundary ∂D of D. Then, using the divergence theorem, it follows from Eq. (2.1) that

$$\frac{d}{dt} \int_D \mathbf{u} d\mathbf{x} + \sum_{j=1}^{d} \int_{\partial D} \mathbf{f}_j(\mathbf{u}) n_j dS = \mathbf{0}. \tag{2.6}$$

This equation is said to be in *integral form*, opposed to (2.1) in *conservative form*. This form is more intuitive to interpret than Eq.(2.1). The time variation of integral of $\mathbf{u}$ over D is equal to the flux loss through the boundary ∂D. In particular, if we take $D = \mathbb{R}^d$, $\mathbf{u}$ should be conserved, as nothing can flow out of this infinite domain in space. In our equation, this can be seen as the boundary integral vanishes:

$$\frac{d}{dt}\int_{\mathbb{R}^d} \mathbf{u} d\mathbf{x} = \mathbf{0}\,. \tag{2.7}$$

Now let

$$\mathbf{A}_j(\mathbf{u}) = \left(\frac{\partial f_{ij}}{\partial u_k}(\mathbf{u})\right)_{1\le i,k\le p} \tag{2.8}$$

be the Jacobian matrix of $\mathbf{f}_j(\mathbf{u})$, for all $j = 1,\ldots,d$, where p is the number of conserved quantities. Since

$$\frac{\partial}{\partial x_j}\mathbf{f}_j = \sum_{k=1}^{p} \frac{\partial \mathbf{f}_j}{\partial u_k}\frac{\partial u_k}{\partial x_j} = \mathbf{A}_j \cdot \frac{\partial}{\partial x_j}\mathbf{u}, \tag{2.9}$$

we can write system (2.1) as

$$\frac{\partial \mathbf{u}}{\partial t} + \sum_{j=1}^{d} \mathbf{A}_j \frac{\partial \mathbf{u}}{\partial x_j} = \mathbf{0}, \qquad \mathbf{x} = (x_1,\ldots,x_d) \in \mathbb{R}^d, t > 0\,, \tag{2.10}$$

We will now restrict ourselves to *hyperbolic* systems of conservation laws, because by definition the Cauchy problem is well posed and has a unique solution for hyperbolic partial differential equations [4]. Furthermore conservation laws of continuum physics are often hyperbolic. System (2.1) is called *hyperbolic* if, for any $\mathbf{u} \in \Omega$ and any $\boldsymbol{\omega} = (\omega_1,\ldots,\omega_d) \in \mathbb{R}^d, \boldsymbol{\omega} \neq \mathbf{0}$, the matrix

$$\mathbf{A}(\mathbf{u},\boldsymbol{\omega}) = \sum_{j=1}^{d} \omega_j \mathbf{A}_j(\mathbf{u}) \tag{2.11}$$

has p real eigenvalues $\lambda_1(\mathbf{u},\boldsymbol{\omega}) \le \lambda_2(\mathbf{u},\boldsymbol{\omega}) \le \ldots \le \lambda_p(\mathbf{u},\boldsymbol{\omega})$ and p linearly independent corresponding eigenvectors $\mathbf{r}_1(\mathbf{u},\boldsymbol{\omega}),\ldots,\mathbf{r}_p(\mathbf{u},\boldsymbol{\omega})$. i.e.,

$$\mathbf{A}(\mathbf{u},\boldsymbol{\omega})\mathbf{r}_k(\mathbf{u},\boldsymbol{\omega}) = \lambda_k(\mathbf{u},\boldsymbol{\omega})\mathbf{r}_k(\mathbf{u},\boldsymbol{\omega})\,, \qquad 1 \le k \le p\,. \tag{2.12}$$

In particular, the system (2.1) is called *strictly hyperbolic* if all eigenvalues $\lambda_k(\mathbf{u},\boldsymbol{\omega})$ are distinct.

Now we will introduce the *Cauchy problem*: Find a solution $\mathbf{u}$ to the system (2.1), satisfying some initial condition

$$\mathbf{u}(\mathbf{x},0) = \mathbf{u}_0(\mathbf{x})\,. \tag{2.13}$$

The *one-dimensional Riemann problem* is a particular one-dimensional case of the Cauchy problem where $\mathbf{u}_0$ consists of a jump discontinuity:

$$\mathbf{u}_0(x) = \begin{cases} \mathbf{u}_l, & x < 0\,, \\ \mathbf{u}_r, & x > 0\,. \end{cases} \tag{2.14}$$

Chapter 3

Weak Solutions

In this chapter it will be shown that, beyond some finite time interval, in general there does not exist a continuously differentiable solution satisfying the Cauchy problem for system (2.1) pointwise. We do this using characteristic curves. Continuously differentiable solutions satisfying the Cauchy problem for (2.1) pointwise are referred to as *classical solutions*. This is the motivation to introduce a broader class of solutions: *weak solutions*.

3.1 Characteristics

We will study the one dimensional scalar case $d = p = 1$. Let the flux function, f, be a continuously differentiable function. The Cauchy problem for system (2.1) is now reduced to

$$\frac{\partial u}{\partial t} + \frac{\partial}{\partial x} f(u) = 0, \tag{3.1}$$

$$u(x,0) = u_0(x). \tag{3.2}$$

Set $a(u) = f'(u)$. Assume u is a classical solution of (3.1), then

$$\frac{\partial u}{\partial t} + a(u)\frac{\partial u}{\partial x} = 0. \tag{3.3}$$

The *characteristic curves* associated with (3.1) are the integral curves of the differential equation:

$$\frac{dx}{dt} = a(u(x(t),t)). \tag{3.4}$$

We will now show that if u is a smooth solution of (3.1), then the characteristic curves are straight lines along which u is constant. This result explains that the characteristic curves propagate the initial conditions u_0 [2]. As a consequence of this, we will see that in general there does not exist a classical solution to the one dimensional Cauchy problem and therefore also not to the Cauchy problem for (2.1).

A characteristic curve passing through the point $(x_0, 0)$ is a solution of

$$\frac{dx}{dt} = a(u(x(t),t)), \tag{3.5}$$

$$x(0) = x_0. \tag{3.6}$$

It exists at least on a small time interval $[0, t_0)$. Along the curve we find

$$du(x(t),t) = \frac{\partial}{\partial t}u(x(t),t)dt + \frac{\partial}{\partial x}u(x(t),t)dx\,, \tag{3.7}$$

$$\frac{du}{dt} = \frac{\partial u}{\partial t} + a(u)\frac{\partial u}{\partial x} = 0 \tag{3.8}$$

Thus u is constant along such a curve and thus equal to $u_0(x_0)$. Therefore $a(u(x(t),t))$ is also constant with time and the characteristic curves are straight lines.

The characteristic curve passing through point $(x_0, 0)$ is given by

$$x = x_0 + t \cdot a(u_0(x_0))\,. \tag{3.9}$$

By setting $u(x,t) = u_0(x_0)$ we see that u has the value of the initial data along the characteristic. This means that the characteristics propagate the information from the initial data. This method of constructing smooth solutions is called the *method of characteristics*.

We will now show that discontinuities can develop after some finite time. Now we make the assumption that there exist two points $x_1 < x_2$ such that the slopes of the characteristic curves are

$$m_1 = \frac{1}{a(u_0(x_1))} < m_2 = \frac{1}{a(u_0(x_2))}\,. \tag{3.10}$$

The curves are described by $t = m_i(x - x_i)$, for $i = 1, 2$. These curves will intersect at some point P. At this point, we find $u = u_0(x_1)$ and $u = u_0(x_2)$. But since $m_1 \neq m_2$, we find that $u_0(x_1) \neq u_0(x_2)$ and thus u has to take on two different values. We conclude that u is not continuous at point P. This intersection occurs at a time t, given by

$$\big(a(u_0(x_1)) - a(u_0(x_2))\big)\, t = x_2 - x_1 > 0\,. \tag{3.11}$$

Now there are two possibilities. The first is that $x \mapsto a(u_0(x))$ is a monotonically increasing function, implying our assumption was not valid. This equation has a solution for $t < 0$, thus we find no intersection for $t > 0$. The other possibility is that $x \mapsto a(u_0(x))$ is not monotonically increasing, therefore our assumption was valid for at least some points x_1 and x_2. In this case we can not determine a classical solution for all $t > 0$, due to the discontinuity at the intersection of the characteristics.

Now that we have shown that discontinuities can develop, we can also determine the critical time T^* up to which a classical solution can exist and be constructed by the method of characteristics. This critical time T^* is the time of first intersection of characteristics. The time of an intersection can be expressed as

$$t = \frac{x_2 - x_1}{a(u_0(x_1)) - a(u_0(x_2))} = -\left(\frac{a(u_0(x_2)) - a(u_0(x_1))}{x_2 - x_1}\right)^{-1}\,. \tag{3.12}$$

The first characteristics to intersect are the ones that lie infinitesimally close to each other, as these 'neighbouring curves' encounter each other first. In this case we recognise that the term within the brackets in our equation reduces to the derivative of a. Therefore if an intersection were to take place, it would happen at a time

$$T = -\left(\frac{d}{dy}a(u_0(y))\right)^{-1}\,. \tag{3.13}$$

An intersection takes place if the derivative $a(u(y))$ is negative at least somewhere. Then the first intersection, $T^* = min(T)$ would be given by

$$T^* = -\left(\min\frac{d}{dy}a(u_0(y))\right)^{-1}\,. \tag{3.14}$$

However, to take into account the case where $a(u_0(y))$ is monotonically increasing, the time T^* up to which a classical solution can be constructed by the method of characteristics is given by

$$T^* = -\frac{1}{\min(0,\alpha)}, \qquad \alpha = \min \frac{d}{dy} a(u_0(y)). \tag{3.15}$$

In summary we have shown that it is possible for characteristics to intersect and therefore that discontinuities can develop. When a discontinuity has developed a classical solution breaks down. The time up to which the classical solution can exist is given by (3.15). We will now show how we can nevertheless analyse the system further using the existence of weak solutions.

3.2 Weak Solutions

We used the method of characteristics to show that a classical solution of (2.1) can exist for a short time interval. However, after a finite time interval discontinuities may develop, not allowing a classical solution. This is the motivation to introduce weak solutions.

Consider the Cauchy problem for (2.1). Let $\mathbf{u}$ be C^1. A C^1 function is a function whose derivative exists and is continuous, but is not necessarily differentiable itself, in other words a continuously differentiable function. Now we introduce a test function $\boldsymbol{\varphi}$. This test function is some continuous differentiable function that falls off fast enough at both spatial infinity, at $t = \infty$ and for $t < 0$, to ensure convergence. Formally $\boldsymbol{\varphi}$ belongs to $\mathbf{C}_0^1(\mathbb{R}^d \times [0,\infty))$, which is the space of C^1 functions with compact support in $\mathbb{R}^d \times [0,\infty)$. We will see an example of such a function in Equation (3.37) and Figure 3.2. We use this test function as follows:

$$\begin{aligned}
&-\int_0^\infty \int_{\mathbb{R}^d} \left\{ \frac{\partial \mathbf{u}}{\partial t} + \sum_{j=1}^d \frac{\partial}{\partial x_j} \mathbf{f}_j(\mathbf{u}) \right\} \boldsymbol{\varphi} d\mathbf{x} dt \\
&= -\int_0^\infty \int_{\mathbb{R}^d} \left(\frac{\partial \mathbf{u}}{\partial t} \right) \boldsymbol{\varphi} d\mathbf{x} dt - \int_0^\infty \int_{\mathbb{R}^d} \left(\sum_{j=1}^d \frac{\partial}{\partial x_j} \mathbf{f}_j(\mathbf{u}) \right) \boldsymbol{\varphi} d\mathbf{x} dt \\
&= -\int_{\mathbb{R}^d} \mathbf{u}(\mathbf{x},t)\boldsymbol{\varphi}(\mathbf{x},t)\Big|_0^\infty d\mathbf{x} + \int_0^\infty \int_{\mathbb{R}^d} \mathbf{u} \frac{\partial \boldsymbol{\varphi}}{\partial t} d\mathbf{x} dt - \int_0^\infty \sum_{j=1}^d \mathbf{f}_j(\mathbf{u}) \boldsymbol{\varphi} \Big|_{\mathbb{R}^d} dt + \int_0^\infty \int_{\mathbb{R}^d} \sum_{j=1}^d \mathbf{f}_j(\mathbf{u}) \frac{\partial \boldsymbol{\varphi}}{\partial x_j} d\mathbf{x} dt \\
&= \int_{\mathbb{R}^d} \mathbf{u}(\mathbf{x},0)\boldsymbol{\varphi}(\mathbf{x},0) d\mathbf{x} + \int_0^\infty \int_{\mathbb{R}^d} \left\{ \mathbf{u} \frac{\partial \boldsymbol{\varphi}}{\partial t} + \sum_{j=1}^d \mathbf{f}_j(\mathbf{u}) \frac{\partial \boldsymbol{\varphi}}{\partial x_j} d\mathbf{x} dt \right\} = 0.
\end{aligned} \tag{3.16}$$

Therefore, all classical solutions of the Cauchy problem, satisfy for any arbitrary and all $\boldsymbol{\varphi} \in \mathbf{C}_0^1(\mathbb{R}^d \times [0,\infty))^p$

$$\int_0^\infty \int_{\mathbb{R}^d} \left\{ \mathbf{u} \frac{\partial \boldsymbol{\varphi}}{\partial t} + \sum_{j=1}^d \mathbf{f}_j(\mathbf{u}) \frac{\partial \boldsymbol{\varphi}}{\partial x_j} \right\} d\mathbf{x} dt + \int_{\mathbb{R}^d} \mathbf{u}_0(\mathbf{x}) \boldsymbol{\varphi}(\mathbf{x},0) d\mathbf{x} = 0. \tag{3.17}$$

With an example we will show, surprisingly, that this equation has more solutions than just the classical solution of the Cauchy problem. Therefore this equation will be used to define *weak solutions*. A function $\mathbf{u}$ is called a *weak solution* of the Cauchy problem for (2.1), if $\mathbf{u}(\mathbf{x},0)$ is a classical solution almost everywhere and satisfies (3.17) for any function $\boldsymbol{\varphi} \in \mathbf{C}_0^1(\mathbb{R}^d \times [0,\infty))^p$.

Let $\boldsymbol{\varphi} \in \mathbf{C}_0^1(\mathbb{R}^d \times (0,\infty))^p$. Integrating Equation (3.17) by parts

$$\int_0^\infty \int_{\mathbb{R}^d} \left\{ \frac{\partial \mathbf{u}}{\partial t} + \sum_{j=1}^d \frac{\partial}{\partial x_j} \mathbf{f}_j(\mathbf{u}) \right\} \boldsymbol{\varphi} d\mathbf{x} dt = 0, \tag{3.18}$$

we see that (2.1) is satisfied pointwise. By choosing $\boldsymbol{\varphi} \in \mathbf{C}_0^1(\mathbb{R}^d \times (0,\infty))^p$, we obtain that any weak solution $\mathbf{u}$ satisfies (2.1) in the sense of distributions on $\mathbb{R}^d \times (0,\infty)$. If a weak solution $\mathbf{u}$ is a C^1 function, then it is also a classical solution. That is because the above equation should hold for any $\boldsymbol{\varphi} \in \mathbf{C}_0^1(\mathbb{R}^d \times (0,\infty))^p$. Therefore a weak solution $\mathbf{u}$ is also a classical solution within any domain where $\mathbf{u}$ is C^1.

3.3 Rankine-Hugoniot Jump Condition

We will give another definition of weak solutions. It is equivalent to the former one, but more applicable. A function is called *piecewise* C^1, if there exists a finite number of smooth orientable surfaces Σ in $\mathbb{R}^d \times [0,\infty)$ outside of which $\mathbf{u}$ is a C^1 function and across which $\mathbf{u}$ has a jump discontinuity. A normal vector of Σ will be denoted by $\mathbf{n} = (n_t, n_{x_1}, \ldots, n_{x_d})^T$. The limits of $\mathbf{u}$ on each side of Σ are denoted by $\mathbf{u}_+$ and $\mathbf{u}_-$.

Let $\mathbf{u}$ be a piecewise C^1 function. Then $\mathbf{u}$ is a *weak solutions* of (2.1) if and only if $\mathbf{u}$ is a classical solution of (2.1) in the domains where $\mathbf{u}$ is C^1, and $\mathbf{u}$ satisfies the Rankine-Hugoniot jump condition along the surfaces of discontinuity:

$$(\mathbf{u}_+ - \mathbf{u}_-)n_t + \sum_{j=1}^{d} (\mathbf{f}_j(\mathbf{u}_+) - \mathbf{f}_j(\mathbf{u}_-))n_{x_j}\,. \tag{3.19}$$

In the previous subsection we have already proven that a weak solution $\mathbf{u}$ is a classical solution of (2.1) in the domains where $\mathbf{u}$ is C^1. The second requirement will now be derived.

Assume that $\mathbf{u}$ is weak solution of (2.1). Let M be a point on the surface of discontinuity Σ and let D be a small ball centred around M. For simplicity we will assume that $\Sigma \cap D$ is the only surface of discontinuity of $\mathbf{u}$ in D. The two open components of D on each side of Σ are denoted by D_+ and D_-. Let $\boldsymbol{\varphi} \in \mathbf{C}_0^1(D)^p$. Recall the divergence theorem.

$$\iiint_V \frac{\partial \mathbf{F}_i}{\partial x_i} dV = \oiint_S \mathbf{F}_i n_i dS\,. \tag{3.20}$$

We will now apply the divergence theorem for $\mathbf{F}_i = \mathbf{f}_i \cdot \boldsymbol{\varphi}$.

$$\begin{aligned}
0 &= + \int_D \left\{ \mathbf{u}\frac{\partial \boldsymbol{\varphi}}{\partial t} + \sum_{j=1}^{d} \mathbf{f}_j(\mathbf{u}) \frac{\partial \boldsymbol{\varphi}}{\partial x_j} \right\} d\mathbf{x}dt \\
&= + \int_{D_+} \left\{ \mathbf{u}\frac{\partial \boldsymbol{\varphi}}{\partial t} + \sum_{j=1}^{d} \mathbf{f}_j(\mathbf{u}) \frac{\partial \boldsymbol{\varphi}}{\partial x_j} \right\} d\mathbf{x}dt + \int_{D_-} \left\{ \mathbf{u}\frac{\partial \boldsymbol{\varphi}}{\partial t} + \sum_{j=1}^{d} \mathbf{f}_j(\mathbf{u}) \frac{\partial \boldsymbol{\varphi}}{\partial x_j} \right\} d\mathbf{x}dt \\
&= - \int_{\Sigma \cap D} \left\{ n_t \mathbf{u}_+ + \sum_{j=1}^{d} n_{x_j} \mathbf{f}_j(\mathbf{u}_+) \right\} \boldsymbol{\varphi} dS - \int_{D_+} \left\{ \frac{\partial \mathbf{u}}{\partial t} + \sum_{j=1}^{d} \frac{\partial}{\partial x_j} \mathbf{f}_j(\mathbf{u}) \right\} \boldsymbol{\varphi} d\mathbf{x}dt \\
&\quad + \int_{\Sigma \cap D} \left\{ n_t \mathbf{u}_- + \sum_{j=1}^{d} n_{x_j} \mathbf{f}_j(\mathbf{u}_-) \right\} \boldsymbol{\varphi} dS - \int_{D_-} \left\{ \frac{\partial \mathbf{u}}{\partial t} + \sum_{j=1}^{d} \frac{\partial}{\partial x_j} \mathbf{f}_j(\mathbf{u}) \right\} \boldsymbol{\varphi} d\mathbf{x}dt\,.
\end{aligned} \tag{3.21}$$

Since $\mathbf{u}$ is a classical solution to (2.1) within D_+ and D_-, the second and fourth integral vanish. The result is

$$- \int_{\Sigma \cap D} \left\{ n_t(\mathbf{u}_+ - \mathbf{u}_-) + \sum_{j=1}^{d} n_{x_j} (\mathbf{f}_j(\mathbf{u}_+) - \mathbf{f}_j(\mathbf{u}_-)) \right\} \boldsymbol{\varphi} dS = 0\,. \tag{3.22}$$

Since this should be satisfied for any $\boldsymbol{\varphi} \in \mathbf{C}_0^1(D)^p$, we obtain exactly Equation (3.19). Therefore if $\mathbf{u}$ is a weak solution of (2.1), the Rankine-Hugoniot conditions are satisfied.

Using the same derivation, without initially setting the equation equal to zero, we find that if a piecewise C^1 function $\mathbf{u}$ is a classical solution of (2.1) in the domains where $\mathbf{u}$ is C^1 and satisfies the Rankine-Hugoniot conditions, then this equation will be equal to zero and thus $\mathbf{u}$ is a weak solution of (2.1).

Introduce the following notation: $[\mathbf{u}] = \mathbf{u}_+ - \mathbf{u}_-$ for the jump of $\mathbf{u}$ across Σ. And $[\mathbf{f}_j(\mathbf{u})] = \mathbf{f}_j(\mathbf{u}_+) - \mathbf{f}_j(\mathbf{u}_-)$ for the jump of $\mathbf{f}_j(\mathbf{u})$ across Σ. We can then write the Rankine Hugoniot jump condition as follows:

$$n_t[\mathbf{u}] + \sum_{j=1}^{d} n_{x_j}[\mathbf{f}_j(\mathbf{u})] = \mathbf{0}. \tag{3.23}$$

3.3.1 Interpretation of the Normal Vector

Let $(n_{x_1}, \ldots, n_{x_d}) \neq \mathbf{0}$. Take the normal vector in the form

$$\mathbf{n} = \begin{pmatrix} -s \\ \boldsymbol{\nu} \end{pmatrix}, \tag{3.24}$$

where $s \in \mathbb{R}$ and $\boldsymbol{\nu} = (\nu_1, \ldots, \nu_d)^T \in \mathbb{R}^d$ is a unit vector. This results in rewriting Equation (3.19) as

$$s[\mathbf{u}] = \sum_{j=1}^{d} \nu_j [\mathbf{f}_j(\mathbf{u})]. \tag{3.25}$$

Note that $\boldsymbol{\nu}$ is normal to the discontinuous surface in $\mathbb{R}^p$ and can therefore interpreted as the direction of propagation. Similarly s may be interpreted as the propagation speed of the discontinuity. Namely, suppose that in one dimension the discontinuity could be parametrized by t and $x = x(t)$. The tangent would be

$$\begin{pmatrix} \frac{\partial x}{\partial t} \\ 1 \end{pmatrix}. \tag{3.26}$$

Then the vector normal to the surface, while keeping the keeping the direction of propagation unchanged is given by

$$\mathbf{n} = \begin{pmatrix} -\frac{\partial x}{\partial t} \\ 1 \end{pmatrix} = \begin{pmatrix} -s \\ 1 \end{pmatrix}. \tag{3.27}$$

We thus see that s is indeed the speed of propagation $\frac{\partial x}{\partial t}$. For the one dimensional ($d = 1$) case we find $s[\mathbf{u}] = [\mathbf{f}(\mathbf{u})]$. Which becomes

$$s[u_i] = [f_i(\mathbf{u})], \qquad 1 \leq i \leq p, \tag{3.28}$$

$$s = \frac{[f_i(\mathbf{u})]}{[u_i]}. \tag{3.29}$$

3.4 Nonuniqueness of Weak Solutions

Weak solutions are in general not unique. This will be shown by an example. Consider the Riemann problem (2.14) for the (scalar, $p = 1$) Burgers' Equation (3.30):

$$\frac{\partial u}{\partial t} + \frac{\partial}{\partial x}\left(\frac{u^2}{2}\right) = 0. \tag{3.30}$$

For $u_l \neq u_r$ we find a weak solution for a single discontinuity propagating at speed

$$s = \frac{\frac{1}{2}(u_r^2 - u_l^2)}{(u_r - u_l)} = \frac{\frac{1}{2}(u_r - u_l)(u_r + u_l)}{(u_r - u_l)} = \frac{1}{2}(u_r + u_l)\,, \tag{3.31}$$

$$u(x,t) = \begin{cases} u_l\,, & x < st\,, \\ u_r\,, & x > st\,. \end{cases} \tag{3.32}$$

A whole family of weak solutions, for $a \geq \max(u_l, -u_r)$, is given by

$$u(x,t) = \begin{cases} u_l\,, & x < s_1 t\,, \\ -a\,, & s_1 t < x < 0\,, \\ a\,, & 0 < x < s_2 t\,, \\ u_r\,, & x > s_2 t\,, \end{cases} \tag{3.33}$$

where

$$s_1 = \frac{1}{2}(u_l - a) < 0\,, \tag{3.34}$$

$$s_2 = \frac{1}{2}(u_r + a) > 0\,. \tag{3.35}$$

If $u_l < u_r$ there is also a classical solution (and thus a weak solution). Notice that $\frac{x}{t}$ is a solution to Burgers' Equation (3.30).

$$u(x,t) = \begin{cases} u_l\,, & x < u_l t\,, \\ \frac{x}{t}\,, & u_l t < x < u_r t\,, \\ u_r\,, & x > u_r t\,, \end{cases} \tag{3.36}$$

is thus a solution to the Riemann problem for Burgers' Equation. By this example we have seen that a solution of the Cauchy Problem is not in general unique.

3.5 Numerical Evaluation of the Non-uniqueness

The non-uniqueness clashes with our mathematical knowledge that first order differential equations have a unique solution up to a single boundary condition. We will now try to understand this non-uniqueness by solving Burgers' Equation numerically. To do so, we smear out any discontinuities by a continuous function which reduces in the limit to the distribution. For instance, the Heaviside step function can be described by the function $\frac{1}{2}\left(1 + \tanh(\epsilon x)\right)$ in the limit $\epsilon \to \infty$. Figure 3.1 gives a graphical illustration of this function for increasing ϵ.

Since the proposed solutions consists of step discontinuities, a smooth approximation can be constructed out of the smoothed out theta functions. As ϵ increases, a smoothed out solution comes closer to the analytical solutions seen in Section 3.4. We thus expect as ϵ increases, the left side of Eq. (3.17) will approach zero. This is done with the numerical integration in Wolfram Mathematica. First, a test function has to be chosen. A test function with compact support in $\mathbb{R} \times (0, \infty)$ is the function

$$f(x,t) = \begin{cases} \exp\left(\frac{1}{x^2-1}\right)\exp\left(\frac{1}{(t-2)^2-1}\right), & |x| < 1, |t-2| < 1\,, \\ 0\,, & \text{otherwise}\,. \end{cases} \tag{3.37}$$

A plot of this function clearly illustrates the compact support, see Figure 3.2.

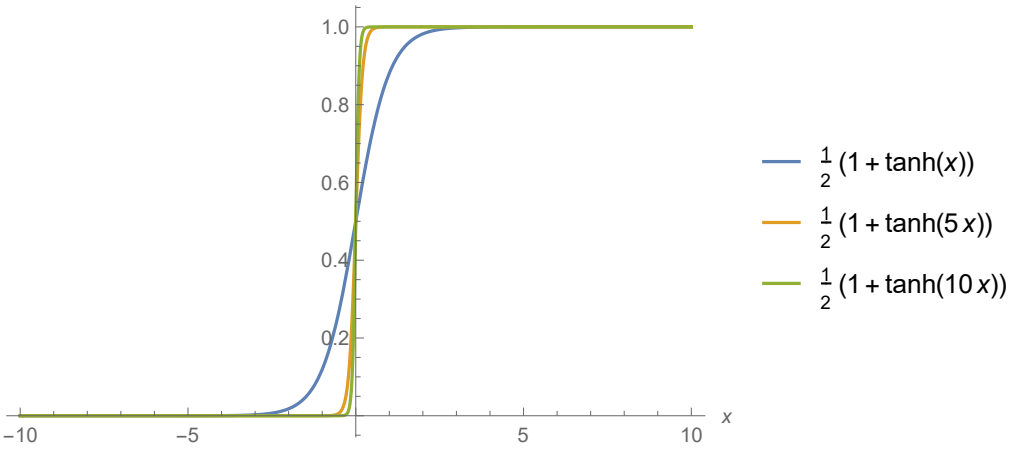

Figure 3.1: *A visual presentation of the function* $\frac{1}{2}\left(1+\tanh\left(\epsilon x\right)\right)$*. We see that this function approaches the Heaviside step function for increasing* ϵ*.*

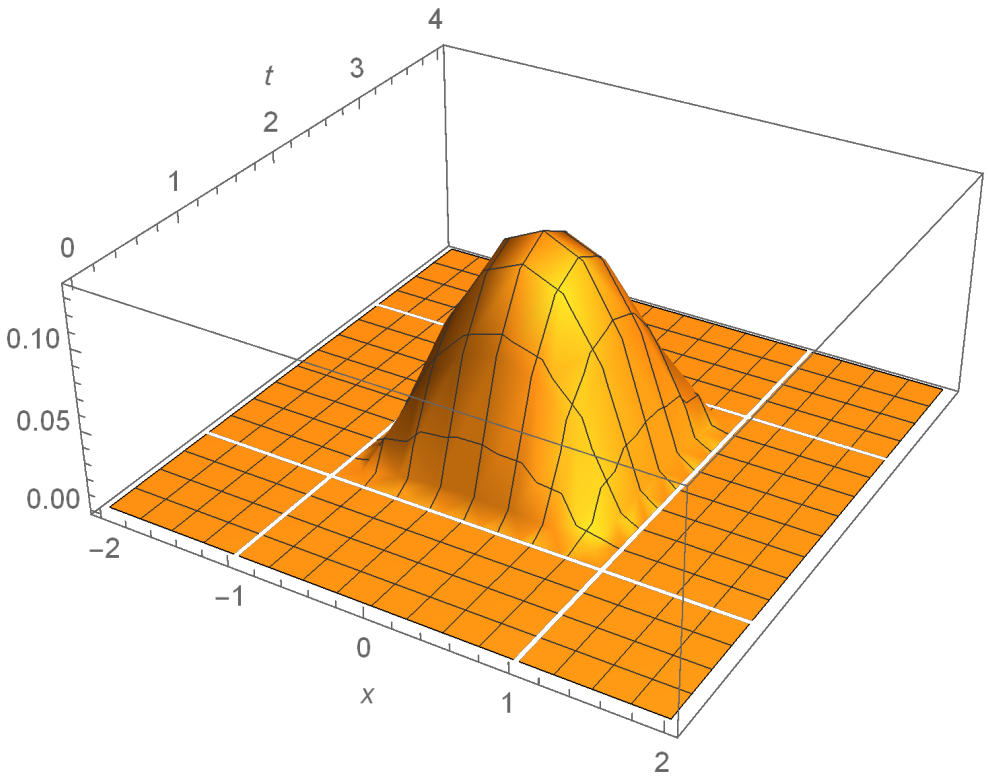

Figure 3.2: *Test function* (3.37)*. The plot illustrates that this function indeed has compact support in* $\mathbb{R}\times(0,\infty)$*.*

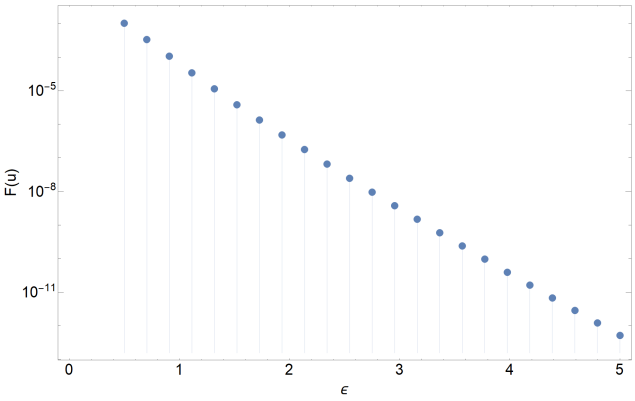

(a) *The integration values as the approximation* (3.38) *approaches* (3.32).

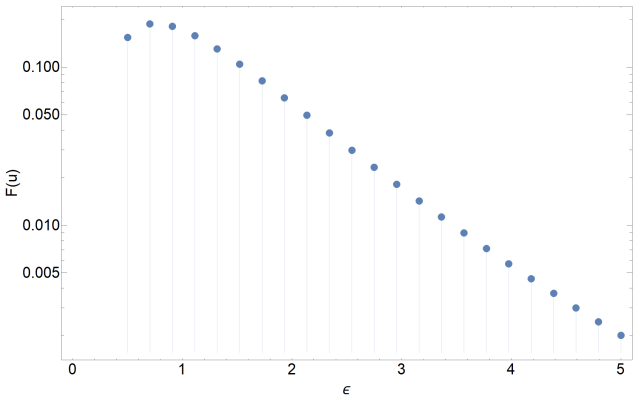

(b) *The integration values as the approximation* (3.39) *approaches* (3.33).

Figure 3.3: *As the approximations to the exact solutions approach the exact solutions, we see that the integral version of Burgers' Equation approaches zero. In other words, the smoothed out versions are not solutions to the conservation equation, but the limits, where the smoothed out functions become a formal distribution, are solutions.*

A smoothed out version of (3.32) is constructed in the following way:

$$\frac{u_l - u_r}{2}\left(1+\tanh\left(\epsilon(-x+t\cdot s)\right)\right)+u_r\,, \tag{3.38}$$

where s is given by Eq. (3.31). Similarly a smoothed version of (3.33) is constructed:

$$\frac{u_l+a}{2}\left(1+\tanh\left(\epsilon(-x+t\cdot s_1)\right)\right)-a+a\left(1+\tanh\left(\epsilon(x)\right)\right)-a+\frac{u_r+a}{2}\left(1+\tanh\left(\epsilon(-x+t\cdot s_2)\right)\right)+u_r\,, \tag{3.39}$$

where s_1 and s_2 are given by (3.34) respectively (3.35). However the smeared out approximations are not solutions to the system.

The integral

$$F(\mathbf{u}) = \int_0^\infty \int_{\mathbb{R}^d} \mathbf{u}\frac{\partial \boldsymbol{\varphi}}{\partial t} + \sum_{j=1}^{d} \mathbf{f}_j(\mathbf{u})\frac{\partial \boldsymbol{\varphi}}{\partial x_j} d\mathbf{x}dt\,, \tag{3.40}$$

for $u_l = 3$ and $u_r = 2$ is computed with numerical integration in Wolfram Mathematica at different values of ϵ for both (3.38) and (3.39). The results are plotted in Figure 3.3.

The results agree with the fact that the integral (3.40) approaches zero for increasing large ϵ. We therefore expect that (3.38) and (3.39) will be weak solutions in the limit where $\epsilon \to \infty$, where they will be equal to (3.32) resp. (3.33).

3.6 Physical Interpretation of the Non-uniqueness

The non-uniqueness seems to arise from the ambiguity in the initial data. The initial data is not defined at $x = 0$. When we look at this from a physical perspective as opposed to the mathematical perspective, we have to notice that there is no such thing as a spatial jump discontinuity in nature. By that I mean a perfect jump discontinuity. Our models may describe jump discontinuities, but these only arise in idealised systems. A good example of an idealised discontinuity that does not exist in real life is a phase transition. We never have a perfect phase change due to all real physical systems being finite (as opposed to the infinite systems for which the perfect phase change is described). Furthermore in quantum mechanics the uncertainty principle prevents perfect discontinuities to exist. Therefore all phenomena we try to describe by jump discontinuities, appear in

nature only as good approximations to a jump discontinuity. The use of a perfect jump condition in our initial data covers up our lack of knowledge of the physical real initial data. Our initial data is an idealisation of multiple possible initial data, namely the different (physical possible) approximations to the step function. It is therefore not at all illogical that we also see multiple solutions arise.

Chapter 4

Entropy Solutions

By a counter example we have seen that a weak solution of the Cauchy Problem is not necessarily unique. In general not all of these solutions necessarily satisfy fundamental physical requirements like the second law of thermodynamics. An additional criterion is required to find the physically relevant solution. For this we need to introduce *entropy*. This chapter will introduce the notion of entropy for the general multidimensional Cauchy problem. In Section 5.2 we will see that the mathematical notion of entropy conditions corresponds to the second law of thermodynamics.

The second law of thermodynamics is an additional law to the conservation laws of mass, momentum and energy. We will therefore start by considering an additional conservation law to our system (2.1):

$$\partial_t U(\mathbf{u}) + \sum_{j=1}^{d} \partial_{x_j} F_j(\mathbf{u}) = 0\,, \tag{4.1}$$

where U and F_j are sufficiently smooth functions. This additional conservation law is satisfied by a solution $\mathbf{u}$ of (2.1) if

$$U'(\mathbf{u})\mathbf{f}_j' = F_j'(\mathbf{u})\,, \tag{4.2}$$

where

$$U' = \nabla U^T = \left(\frac{\partial U}{\partial u_1}, \frac{\partial U}{\partial u_2}, \cdots, \frac{\partial U}{\partial u_p}\right) \text{and } F_j' = \nabla F_j^T = \left(\frac{\partial F_j}{\partial u_1}, \frac{\partial F_j}{\partial u_2}, \cdots, \frac{\partial F_j}{\partial u_p}\right), \tag{4.3}$$

and $\mathbf{f}_j$ is denoted by

$$\mathbf{f}_j' = \mathbf{A}_j = \left(\frac{\partial f_{ij}}{\partial u_k}\right)_{1\le i,k\le p}. \tag{4.4}$$

Namely,

$$0 = U'(\mathbf{u})\left(\frac{\partial \mathbf{u}}{\partial t} + \sum_{j=1}^{d} \frac{\partial}{\partial x_j}\mathbf{f}_j(\mathbf{u})\right) = U'(\mathbf{u})\left(\frac{\partial \mathbf{u}}{\partial t} + \sum_{j=1}^{d} \mathbf{f}_j'(\mathbf{u})\frac{\partial \mathbf{u}}{\partial x_j}\right) = U'(\mathbf{u})\frac{\partial \mathbf{u}}{\partial t} + \sum_{j=1}^{d} U'(\mathbf{u})\mathbf{f}_j'(\mathbf{u})\frac{\partial \mathbf{u}}{\partial x_j}\,. \tag{4.5}$$

Now substitute (4.2),

$$U'(\mathbf{u})\frac{\partial \mathbf{u}}{\partial t} + \sum_{j=1}^{d} F_j'(\mathbf{u})\frac{\partial \mathbf{u}}{\partial x_j} = \frac{\partial U}{\partial t} + \sum_{j=1}^{d} \frac{\partial}{\partial x_j} F_j(\mathbf{u}) = 0\,, \tag{4.6}$$

which is exactly (4.1). Equation (4.2) will be used to define *entropy*. A convex function U is called an *entropy* of the system (2.1) if there exists d functions $F_j(\mathbf{u})$ such that (4.2) holds. F_j are called *entropy fluxes*.

It has been shown that if (4.2) holds, then any classical solution $\mathbf{u}$ of (2.1) satisfies the additional conservation law (4.1). This is not true for a weak solution. A weak solution of (2.1) should satisfy the Rankine-Hugoniot jump condition (3.19) along Σ. A solution of the additional conservation law (4.1) should satisfy the corresponding jump condition:

$$n_t [U(\mathbf{u})] + \sum_{j=1}^{d} n_{x_j} [F_j(\mathbf{u})] . \tag{4.7}$$

This additional jump condition however is not in general compatible with the Rankine-Hugoniot jump condition.

It can be shown that, as is done in [3], if one introduces a viscous perturbation to (2.1) and takes the limit in which this perturbation vanishes, then weak solutions of this system of conservation laws will satisfy

$$\frac{\partial}{\partial t} U(\mathbf{u}) + \sum_{j=1}^{d} \frac{\partial}{\partial x_j} F_j(\mathbf{u}) \leq 0 . \tag{4.8}$$

Note however, that the additional conservation law (4.1) is not yet satisfied, due to the inequality. This inequality will be used to define an *entropy solution* in terms of an additional jump condition. A weak solution $\mathbf{u}$ is called an *entropy solution* if it additionally satisfies the jump inequality:

$$n_t \left[U(\mathbf{u})\right] + \sum_{j=1}^{d} n_{x_j} \left[F_j(\mathbf{u})\right] \leq 0 , \tag{4.9}$$

along the surfaces of discontinuity, for $\frac{\mathbf{n}}{|\mathbf{n}|}$ is the outward unit normal vector pointing in the D_+ direction. This equation can be referred to as the entropy condition. In the one dimensional case this becomes

$$s[U(\mathbf{u})] \geq [F(\mathbf{u})] , \tag{4.10}$$

where s is the propagation speed of the discontinuity. The uniqueness of an entropy solution has been shown by S. N. Kružkov [5].

Chapter 5

The Lax Entropy Conditions

We recall what we have learned so far, and we consider the specific case of one space dimension. In this particular case, we will derive the Lax entropy conditions and see how these relate to the second law of thermodynamics. Furthermore, we will also relate the more general abstract entropy condition of the previous chapter to the thermodynamic entropy.

5.1 Characteristic Curves in One Space Dimension

In one space dimension we have the system of conservation laws

$$\partial_t \mathbf{u} + \partial_x \mathbf{f}(\mathbf{u}) = 0, \quad x \in \mathbb{R}, t > 0. \tag{5.1}$$

This equation can also be written as

$$\partial_t \mathbf{u} + \mathbf{A}(\mathbf{u})\partial_x \mathbf{u} = 0, \quad x \in \mathbb{R}, t > 0, \tag{5.2}$$

where

$$\mathbf{A}(\mathbf{u}) = \left(\frac{\partial f_i}{\partial u_j}(\mathbf{u}) \right)_{1 \le i,j \le p} \tag{5.3}$$

is the Jacobian matrix of $\mathbf{f}$. Assume that the system is strictly hyperbolic. Then for any $\mathbf{u}$, the Jacobi matrix $\mathbf{A}(\mathbf{u})$ has p distinct eigenvalues

$$\lambda_1(\mathbf{u}) < \lambda_2(\mathbf{u}) < \ldots < \lambda_p(\mathbf{u}). \tag{5.4}$$

The 'right' eigenvector associated with the eigenvalue $\lambda_k(\mathbf{u})$ is denoted by $\mathbf{r}_k(\mathbf{u})$, e.g.

$$\mathbf{A}(\mathbf{u})\mathbf{r}_k(\mathbf{u}) = \lambda_k(\mathbf{u})\mathbf{r}_k(\mathbf{u}). \tag{5.5}$$

The 'left' eigenvector associated with the eigenvalue $\lambda_k(\mathbf{u})$ is denoted by $\mathbf{l}_k(\mathbf{u})$, e.g.

$$\mathbf{l}_k(\mathbf{u})^T \mathbf{A}(\mathbf{u}) = \lambda_k(\mathbf{u})\mathbf{l}_k(\mathbf{u})^T. \tag{5.6}$$

So $\mathbf{l}_k(\mathbf{u})$ is a 'right' eigenvector of $\mathbf{A}(\mathbf{u})^T$. Furthermore $\mathbf{l}_j(\mathbf{u}) \cdot \mathbf{r}_k(\mathbf{u}) = \delta_k^j$. Namely,

$$\mathbf{l}_j(\mathbf{u})^T \mathbf{A}(\mathbf{u})\mathbf{r}_k(\mathbf{u}) = \lambda_k(\mathbf{u})\mathbf{l}_j(\mathbf{u})^T \mathbf{r}_k(\mathbf{u}), \tag{5.7}$$

$$\mathbf{l}_j(\mathbf{u})^T \mathbf{A}(\mathbf{u})\mathbf{r}_k(\mathbf{u}) = \lambda_j(\mathbf{u})\mathbf{l}_j(\mathbf{u})^T \mathbf{r}_k(\mathbf{u}). \tag{5.8}$$

Thus

$$\lambda_k(\mathbf{u})\mathbf{l}_j(\mathbf{u})^T\mathbf{r}_k(\mathbf{u}) = \lambda_j(\mathbf{u})\mathbf{l}_j(\mathbf{u})^T\mathbf{r}_k(\mathbf{u})\,. \tag{5.9}$$

And since all eigenvalues are real and distinct we find that $\mathbf{l}_j(\mathbf{u})\cdot\mathbf{r}_k(\mathbf{u}) = 0$ for $j \neq k$. Now $\mathbf{l}_j(\mathbf{u})\cdot\mathbf{r}_j(\mathbf{u}) = 1$, is choice of normalisation.

We will also find a simple expression for the characteristic curves in one space dimension. We start by rewriting

$$\partial_t\mathbf{u} + \mathbf{A}(\mathbf{u})\partial_x\mathbf{u} = 0\,, \tag{5.10}$$

as

$$\mathbf{l}_k(\mathbf{u})^T\left(\partial_t\mathbf{u} + \lambda_k(\mathbf{u})\partial_x\mathbf{u}\right) = 0\,, \quad 1 \leq k \leq p\,. \tag{5.11}$$

Now we see that the integral curves of the system are

$$\frac{dx}{dt} = \lambda_k(\mathbf{u}(x,t))\,. \tag{5.12}$$

The characteristic curves (3.9) are thus given by

$$x = x_0 + t\cdot\lambda_k(\mathbf{u}(x,t)) = x_0 + t\cdot\lambda_k(\mathbf{u}_0(x_0))\,. \tag{5.13}$$

We will now discuss the three classes of solutions to the Riemann problem. Recall that u is constant along the characteristic curves. Therefore these characteristic curves propagate the initial data, since the characteristic line passing through $(x_0, 0)$ propagates the value $\mathbf{u}_0(x_0)$ along the curve. The characteristics are straight lines with slope $\frac{dt}{dx} = \frac{1}{\lambda_k}$ in the (x,t)-plane. Now consider the case where $\lambda_k(\mathbf{u}_l) < \lambda_k(\mathbf{u}_r)$. In this particular case the characteristics on the left side of the discontinuity are steeper than the characteristics on the right side of the discontinuity. The different characteristics will therefore not intersect. In this case there is a unique classical solution. In this type of solution the discontinuity is smeared out. This type of solution will be referred to as an *expansion fan* or a *rarefaction wave*. The second case is when $\lambda_k(\mathbf{u}_l) = \lambda_k(\mathbf{u}_r)$. Since the slopes are equal, the characteristics will not intersect. In contrast to the expansion fan, in this case discontinuity is not smeared out, but rather stays intact. As the initial data propagates with a speed $\lambda_k(\mathbf{u}_l) = \lambda_k(\mathbf{u}_r) = s$, the discontinuity will also propagate at a speed s. This type of solution is referred to as a *contact discontinuity*. The last case is when $\lambda_k(\mathbf{u}_l) > \lambda_k(\mathbf{u}_r)$. In this case the characteristics on the left of the discontinuity are less steep than the characteristics on the right of the discontinuity, causing them to intersect. In this case we have a weak solution in which a discontinuity propagates with speed s. In the next section we will discuss this type of solution which is referred to as a *shock wave*.

5.2 Lax Entropy conditions

We will now consider the shock waves. Take a point along the line of discontinuity, call this point P. Furthermore consider a shock wave travelling with speed s. In point P we can construct all characteristic curves through this point, simply by calculating $\lambda_k(\mathbf{u})$ for all $1 \leq k \leq p$. However due to the ambiguity, we can construct these for both $\mathbf{u} = \mathbf{u}_l$ and $\mathbf{u} = \mathbf{u}_r$. The characteristics are straight lines with slope $\frac{dx}{dt} = \lambda_k$. Consider the characteristics for $\mathbf{u} = \mathbf{u}_l$. If this slope is steeper than the slope of the discontinuity, the characteristic can be traced back to the point $t = 0$ where it has value $\mathbf{u} = \mathbf{u}_l$, see Fig. 5.1. The characteristics with respect to $\mathbf{u}_l$ which have a smaller slope than the discontinuity can only be evaluated at a future time t. These characteristics can not be traced back to the point $t = 0$ an thus not to the initial data. However we have seen that these characteristics propagate initial data. Therefore these characteristics require additional boundary conditions. If in point P

$$\lambda_1(\mathbf{u}_l) < \ldots < \lambda_k(\mathbf{u}_l) < s < \lambda_{k+1}(\mathbf{u}_l) < \ldots < \lambda_p(\mathbf{u}_l)\,, \tag{5.14}$$

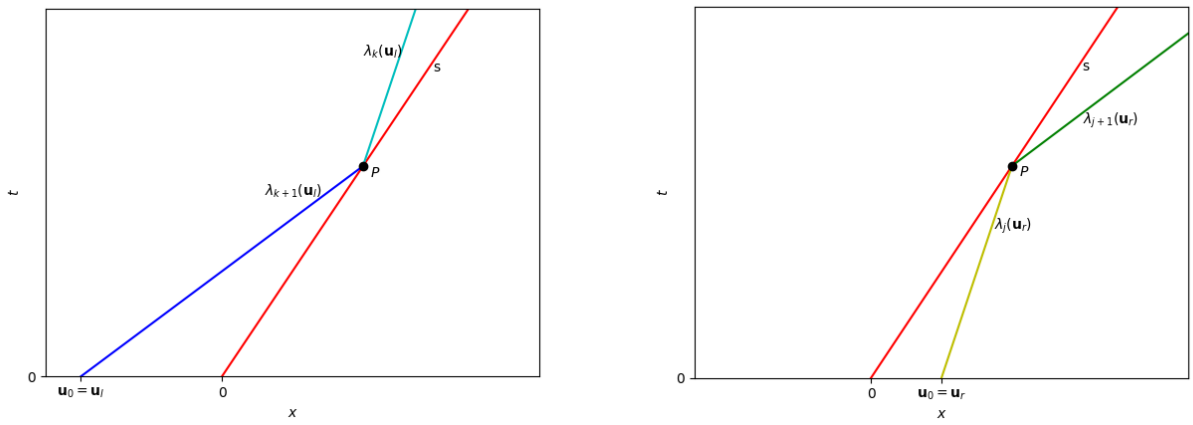

(a) ***(b)***

Figure 5.1: *The characteristics running into the shock wave and appearing from the wave. The red curve denotes the shock wave. In (a) the blue curves represent the characteristics from and to the left, in (b) the green curves represent the characteristics from and to the right.*

where s denotes the slope of the discontinuity, k characteristics are less steep and can not be connected to the initial data. k boundary conditions are required.

Similarly we can construct the characteristics with respect to $\mathbf{u}_r$. These are either steeper than s and can only be evaluated for future times, or less steep which means they can be traced back to the initial data. If in point P

$$\lambda_1(\mathbf{u}_r) < \ldots < \lambda_j(\mathbf{u}_r) < s < \lambda_{j+1}(\mathbf{u}_r) < \ldots < \lambda_p(\mathbf{u}_r)\,, \tag{5.15}$$

$p-j$ characteristics can not be connected to the initial data and thus $p-j$ additional boundary conditions are needed. This gives a total of $k+p-j$ required boundary conditions. Now we should realise that we already have some boundary conditions, namely the Rankine-Hugoniot jump conditions. The Rankine-Hugoniot jump conditions consist of p equations. However, we need one of them to determine s. Therefore, after eliminating s, we have $p-1$ boundary conditions.

The Lax entropy conditions tell us that the amount of boundary conditions required by the characteristics should be equal to the amount of boundary conditions provided,

$$k+p-j = p-1\,. \tag{5.16}$$

Therefore if we set $j = k+1$, we do not miss any information to construct all characteristics and simultaneously all the boundary conditions can be satisfied.

This leads us to the Lax entropy conditions. A shock wave is only allowed if it satisfies the Lax entropy conditions. The Lax entropy conditions are satisfied if there exists a $k \in \{1,2,\ldots,p\}$, such that we have

$$\lambda_{k-1}(\mathbf{u}_l) < s < \lambda_k(\mathbf{u}_l)\,, \quad \lambda_k(\mathbf{u}_r) < s < \lambda_{k+1}(\mathbf{u}_r)\,. \tag{5.17}$$

Note that this is consistent with $\lambda_k(\mathbf{u}_l) > \lambda_k(\mathbf{u}_r)$, which was the case of the shock wave. Since this case required a weak solution, the above equations will pick the physical relevant solution from all possible weak solution. In the following section we will see why this is the case.

5.3 Physical Interpretation of the Lax Entropy Conditions

We want to show that the mathematical notion of these entropy conditions is in the applications in physics equivalent to the second law of thermodynamics.

5.3.1 Information

For our solution to be consistent with all boundary conditions, we need at least the same number of degrees of freedom as the number of boundary conditions to be able to impose those boundary conditions. Thus the number of required boundary conditions should be at least as large as the number of boundary conditions we that we have by the jump conditions. However if we have less boundary conditions from the jump conditions than the number of required boundary conditions, we miss information. This would mean information has to be created.

5.3.2 Thermodynamic Notion of Entropy of Particles Passing Crossing the Shock

Consider the compressible Euler equations in one dimension

$$\partial_t \rho + \partial_x \rho u = 0, \tag{5.18}$$

$$\partial_t \rho u + \partial_x \left(\rho u^2 + p \right) = 0, \tag{5.19}$$

$$\partial_t \rho e + \partial_x \left(\left(\rho e + p \right) u \right) = 0. \tag{5.20}$$

Where ρ is the mass density, u is the flux velocity, p the pressure, $e = \varepsilon + \frac{u^2}{2}$ is the specific total energy, ε is the specific internal energy.

Equation (5.19) can be written as

$$u\partial_t \rho + \rho \partial_t u + u\rho \partial_x u + u\partial_x \rho u + \partial_x p = 0. \tag{5.21}$$

Substitute (5.18) into this equation to find

$$\partial_t u + u\partial_x u + \frac{1}{\rho}\partial_x p = 0. \tag{5.22}$$

Equation (5.20) can be written as

$$\rho \partial_t \varepsilon + \partial_t \rho \frac{u^2}{2} + \varepsilon \partial_t \rho + \rho u \partial_x \varepsilon + \varepsilon \partial_x \rho u + \partial_x \left(\rho \frac{u^2}{2} u + pu \right) = 0. \tag{5.23}$$

Substitute (5.18) into this equation to find

$$\rho \left(\partial_t \varepsilon + u\partial_x \varepsilon + \frac{p}{\rho}\partial_x u \right) + \partial_t \rho \frac{u^2}{2} + \partial_x \rho \frac{u^2}{2} u + u\partial_x p = 0, \tag{5.24}$$

$$\rho \left(\partial_t \varepsilon + u\partial_x \varepsilon + \frac{p}{\rho}\partial_x u \right) + u\partial_t \rho u - \frac{u^2}{2}\partial_t \rho + u\partial_x \rho u^2 - \frac{u^2}{2}\partial_x \rho u + u\partial_x p = 0. \tag{5.25}$$

Substitute (5.18) and (5.19) to find

$$\partial_t \varepsilon + u\partial_x \varepsilon + \frac{p}{\rho}\partial_x u = 0. \tag{5.26}$$

Therefore, the Euler equations can be written as

$$\partial_t \rho + u\partial_x \rho + \rho \partial_x u = 0, \tag{5.27}$$

$$\partial_t u + u\partial_x u + \frac{1}{\rho}\partial_x p = 0, \tag{5.28}$$

$$\partial_t \varepsilon + u\partial_x \varepsilon + \frac{p}{\rho}\partial_x u = 0. \tag{5.29}$$

Consider the general form of conservation laws as in (5.2). Then

$$\partial_t \mathbf{u} + \mathbf{A}(\mathbf{u})\partial_x \mathbf{u} = 0\,, \quad x \in \mathbb{R}, t > 0\,, \tag{5.30}$$

where

$$\mathbf{u} = \begin{pmatrix} \rho \\ u \\ \varepsilon \end{pmatrix}, \quad \mathbf{A} = \begin{pmatrix} u & \rho & 0 \\ \frac{1}{\rho}\frac{\partial p}{\partial \rho} & u & 0 \\ 0 & \frac{p}{\rho} & 0 \end{pmatrix}. \tag{5.31}$$

Then finding the eigenvalues of $\mathbf{A}$,

$$(u-\lambda)\left((u-\lambda)^2 - \frac{\partial p}{\partial \rho}\right) = 0\,. \tag{5.32}$$

$$\lambda_1 = u - c\,, \quad \lambda_2 = u\,, \quad \lambda_3 = u + c\,, \tag{5.33}$$

where

$$c = \sqrt{\frac{\partial p}{\partial \rho}}\,, \tag{5.34}$$

is the sound speed.

Suppose we want to solve the Riemann problem for compressible flow. We can apply the Lax entropy conditions to find which shocks are allowed. In this case we find two possible shock waves, a left moving one and a right moving one. Consider the right moving shock. It has to satisfy the following inequalities

$$u_l < s < u_l + c_l\,, \tag{5.35}$$

$$u_r + c_r < s\,, \tag{5.36}$$

where c_l and c_r are the sound speeds on either side of the shock wave. The shock speed is larger than the flow speed on both sides of the shock. Therefore the particles cross the shock from the right to the left [1]. More specifically, the conditions tell us that the shock is supersonic with respect to the right and subsonic with respect to the left. Also notice that this can only be satisfied if $u_r + c_r < u_l + c_l$. If this cannot be satisfied the right moving shock is not allowed as it would violate the entropy conditions.

Now we will show that this is equivalent to the second law of thermodynamics. To do this we will closely follow the discussion of Courant and Friedrichs [6, Chapter 65] and Weyl [7]. We will see that as a particle crosses a shock, the entropy increases. Consider a column around the surface of discontinuity, with ends $a_l(t)$ and $a_r(t)$. $a_l(t)$ and $a_r(t)$ denote the position of the particles that define the ends of the column. Therefore $\dot{a_l}(t) = u_l$ and $\dot{a_r}(t) = u_r$ are the flow velocities on either side of the discontinuity. The position of the surface of discontinuity is denoted by $\xi(t)$. Then $\dot{\xi}(t) = s$ is the shock speed.

Consider the three conservation laws

$$\frac{d}{dt}\int_{a_l(t)}^{a_r(t)} \rho dx = 0\,, \tag{5.37}$$

$$\frac{d}{dt}\int_{a_l(t)}^{a_r(t)} \rho u dx = p(a_0,t) - p(a_1,t)\,, \tag{5.38}$$

$$\frac{d}{dt}\int_{a_l(t)}^{a_r(t)} \rho\left(\frac{1}{2}u^2 + \varepsilon\right) dx = p(a_0,t)u(a_0,t) - p(a_1,t)u(a_1,t)\,. \tag{5.39}$$

Now use Leibniz integral rule to perform the differentiation under the integral for some quantity $U(x,t)$.

$$\frac{d}{dt}\int_{a_l(t)}^{a_r(t)} U(x,t)dx = \frac{d}{dt}\int_{a_l(t)}^{\xi(t)} U(x,t)dx + \frac{d}{dt}\int_{\xi(t)}^{a_r(t)} U(x,t)dx \tag{5.40}$$

$$= U_l s - U(a_l,t)u_l + \int_{a_l(t)}^{\xi(t)} \frac{\partial}{\partial t}U(x,t)dx + U(a_r,t)u_r - U_r s + \int_{\xi(t)}^{a_r(t)} \frac{\partial}{\partial t}U(x,t)dx\,. \tag{5.41}$$

U_l and U_r are the left respectively right limit of $U(x,t)$ as x approaches $\xi(t)$. Now we take the limit where the length of the column approaches zero by letting $a_l(t)$ and $a_r(t)$ approach $\xi(t)$. Both integrals will vanish and $U(a_l,t) \to U_l$ and $U(a_r,t) \to U_r$. We thus obtain

$$\lim_{(a_l,a_r)\to(\xi^-,\xi^+)} \frac{d}{dt}\int_{a_l(t)}^{a_r(t)} U(x,t)dx = U_r(u_r - s) - U_l(u_l - s)\,. \tag{5.42}$$

We substitute $v_l = u_l - s$ and $v_r = u_r - s$ to find

$$\rho_1 v_1 - \rho_0 v_0 = 0\,, \tag{5.43}$$

$$(\rho_1 u_1)v_1 - (\rho_0 u_0)v_0 = p_0 - p_1\,, \tag{5.44}$$

$$\rho_1(\frac{1}{2}u_1^2\varepsilon_1)v_1 - \rho_0(\frac{1}{2}u_0^2\varepsilon_0)v_0 = p_0u_0 - p_1u_1\,, \tag{5.45}$$

where 0 can denote r and 1 can denote l or vice versa. To find a weak solution to the conservation laws, the above jump conditions need to be satisfied. Using the specific volume $\tau = \frac{1}{\rho}$ and $\rho_1 v_1 = \rho_0 v_0 = m$, we can derive the following from the above equations

$$m(\frac{1}{2}v_0^2 + \varepsilon_0 + p_0\tau_0) = m(\frac{1}{2}v_1^2 + \varepsilon_1 + p_1\tau_1)\,. \tag{5.46}$$

If we have $m \neq 0$ we can rewrite this as

$$\frac{1}{2}(v_0^2 - v_1^2) = \varepsilon_1 - \varepsilon_0 + p_1\tau_1 - p_0\tau_0\,. \tag{5.47}$$

Equation (5.44) can be rewritten as

$$p_1 - p_0 = m(v_0 - v_1)\,. \tag{5.48}$$

From this equation we can find that

$$(\tau_0 + \tau_1)(p_1 - p_0) = m(\tau_0 + \tau_1)(v_0 - v_1) = (v_0 + v_1)(v_0 - v_1) = v_0^2 - v_1^2\,. \tag{5.49}$$

Substitute this into (5.47) to find

$$\frac{1}{2}(\tau_0 + \tau_1)(p_1 - p_0) = \varepsilon_1 - \varepsilon_0 + p_1\tau_1 - p_0\tau_0\,. \tag{5.50}$$

This equation can be rewritten as

$$\varepsilon_1 - \varepsilon_0 = \frac{1}{2}(p_1 + p_0)(\tau_0 - \tau_1)\,. \tag{5.51}$$

This equation is used to define the Hugoniot function

$$H(\tau,p) = \varepsilon(\tau,p) - \varepsilon(\tau_0,p_0) + \frac{1}{2}(p + p_0)(\tau - \tau_0). \tag{5.52}$$

All states (τ,p) that can be on the other side of the shock wave of state (τ_0,p_0), while being consistent with the Rankine-Hugoniot jump conditions, should satisfy $H(\tau,p) = 0$. The curve $H(\tau,p) = 0$ in (τ,p)-space is called

the Hugoniot curve. We will now use the Hugoniot function to show that the specific entropy S increases as the specific volume τ decreases. For this we will need the following three assumptions:

$$-\rho^2 c^2 = \frac{\partial}{\partial \tau} p(\tau, S) < 0, \tag{5.53}$$

$$\frac{\partial^2}{\partial \tau^2} p(\tau, S) > 0, \tag{5.54}$$

$$\frac{\partial}{\partial S} p(\tau, S) > 0. \tag{5.55}$$

The first of which states that pressure increases with increasing density for constant entropy, which is considered a fundamental property of all actual media. The second assumption states that for constant entropy, the pressure is a concave function of τ. The third assumption states that for constant specific volume, the pressure increases with entropy. These basic assumptions can be derived for polytropic media [6].

Since $H = 0$ along the Hugoniot curve, we require $dH = 0$. Using the relation $TdS = d\varepsilon + pd\tau$, where T is the temperature, we find

$$\begin{aligned} dH &= d\varepsilon + \frac{1}{2}(\tau - \tau_0)dp + \frac{1}{2}(p + p_0)d\tau \\ &= TdS - pd\tau + \frac{1}{2}(\tau - \tau_0)dp + \frac{1}{2}(p + p_0)d\tau \\ &= TdS + \frac{1}{2}(\tau - \tau_0)dp - \frac{1}{2}(p - p_0)d\tau = 0. \end{aligned} \tag{5.56}$$

At $p = p_0$ and $\tau = \tau_0$ this yields $TdS = 0$ for all T, thus

$$dS = 0. \tag{5.57}$$

Differentiate again, to find

$$0 = 2d(TdS) + (\tau - \tau_0)d^2 p - (p - p_0)d^2 \tau \tag{5.58}$$

At $p = p_0$ and $\tau = \tau_0$ this yields

$$0 = d(TdS) = dTdS + Td^2 S = Td^2 S \text{ for all } T. \tag{5.59}$$

Therefore

$$dS^2 = 0. \tag{5.60}$$

Differentiate again, to find

$$0 = 2d^2(TdS) + d\tau d^2 p - d^2 \tau dp + (\tau - \tau_0)d^3 p - (p - p_0)d^3 \tau \tag{5.61}$$

At $p = p_0$ and $\tau = \tau_0$ this yields

$$0 = 2Td^3 S + d\tau d^2 p - d^2 \tau dp, \tag{5.62}$$

for all T. Now using the two assumptions (5.53) and (5.54), we find that $d^3 S > 0$ for $d\tau < 0$ in the point $p = p_0$ and $\tau = \tau_0$. To show that S increases as τ decreases along the whole curve, we can show that S is a monotone decreasing function of τ along the Hugoniot curve ($H(\tau, p) = 0$). This is true if $dS \neq 0$ everywhere except in (τ_0, p_0). Suppose there was another point (τ_1, p_1) on the Hugoniot curve at which $dS = 0$. Then according to (5.56), we would find that in this point

$$\frac{d\tau}{dp} = \frac{(\tau_1 - \tau_2)}{(p_1 - p_2)} \tag{5.63}$$

Therefore the tangent of the Hugoniot curve in the point (τ_1, p_1) is equal to the straight curve between (τ_0, p_0) and (τ_1, p_1), since both curves have equal derivatives there. We will now parametrize the straight curve with a parameter ξ. Along this curve we find $dp = a d\xi$ and $d\tau = b d\xi$, where $a = p_1 - p_0$ and $b = \tau_1 - \tau_0$. Then we find along this curve according to (5.56) that $dH = T dS$. Now we note that the Hugoniot curve $(H(\tau, p) = 0)$ can not coincide with the straight curve. This is because along the whole Hugoniot curve we have $dH = 0$ which this would then mean that $dS = 0$ along the whole curve, but this contradicts with the fact that we found that in point (τ_0, p_0) S increases with τ. Therefore the Hugoniot curve does not coincide with the straight curve. Nevertheless we can still calculate the value of H along the straight curve. Since $H(\xi)$ vanishes at two points along this curve, there needs to be at least one extreme point of $H(\xi)$ on this curve. According to $dH = T dS$ on this curve, $\frac{dS}{d\xi}$ should also vanish at this extreme. We will now show that this extreme is a maximum.

$$\partial_\xi S = b\partial_\tau S + a\partial_p S, \tag{5.64}$$

$$\partial_{\xi\xi} S = b^2\partial_{\tau\tau} S + 2ab\partial_{\tau p} S + a^2\partial_{pp} S. \tag{5.65}$$

Using $\frac{\partial_\tau S}{\partial_p S} = -\frac{a}{b}$ we find

$$\partial_{\xi\xi} S = \frac{a^2}{(\partial_\tau S)^2}\left(\partial_{\tau\tau} S\,(\partial_p S)^2 + 2\partial_{\tau p} S\,\partial_\tau S\,\partial_p S + \partial_{pp} S\,(\partial_\tau S)^2\right) \tag{5.66}$$

Now from $S = S(\tau, p) = S(\tau, p(\tau, S))$ we find that $\partial_p S \partial_S p(\tau, S) = 1$. Therefore, according to (5.55) we find $\partial_p S > 0$. In the point (τ_0, p_0) we have $0 = \partial_\tau S + \partial_p S \partial_\tau p(\tau, S)$, which leads according to (5.53) to $\partial_\tau S > 0$. Differentiate once more and use $\partial_\tau p = -\frac{\partial_\tau S}{\partial_p S}$ to find

$$\begin{aligned}\frac{d}{d\tau}(\partial_\tau S + \partial_p S\partial_\tau p) &= \partial_{\tau\tau} S + 2\partial_{p\tau} S\partial_\tau p + \partial_{pp} S(\partial_\tau p)^2 + \partial_p S\partial_{\tau\tau} p \\ &= \frac{1}{(\partial_p S)^2}\left(\partial_{\tau\tau} S(\partial_p S)^2 - 2\partial_{p\tau} S\partial_\tau S\partial_p S + \partial_{pp} S(\partial_\tau S)^2 + (\partial_p S)^3\partial_{\tau\tau} p\right) = 0.\end{aligned} \tag{5.67}$$

Now from assumption (5.54) and $\partial_p S > 0$ follows that

$$\partial_{\tau\tau} S(\partial_p S)^2 - 2\partial_{p\tau} S\partial_\tau S\partial_p S + \partial_{pp} S(\partial_\tau S)^2 < 0. \tag{5.68}$$

Compare this with Equation (5.66). We can now conclude that $\partial_{\xi\xi} S$ is negative and therefore $S(\xi)$ has exactly a maximum along the straight curve. Specifically we see that S has only one stationary point $(dS = 0)$ along this straight curve. This then implies

$$\frac{dS}{d\xi} > 0 \text{ at } (\tau_0, p_0), \tag{5.69}$$

$$\frac{dS}{d\xi} < 0 \text{ at } (\tau_1, p_1). \tag{5.70}$$

This contradicts with that fact that $dS = 0$ in point (τ_1, p_1). We can conclude that there does not exist another point than (τ_1, p_1) along the Hugoniot curve at which $dS = 0$ and thus the straight line can not be tangent to the Hugoniot curve. This means that we can conclude that along the whole Hugoniot curve, S increases as τ decreases. All that is left to do is show that as particles cross the shock, τ decreases. let (τ_0, p_0) be the state on one side of the shock and (τ_1, p_1) the state on the other side. Although the straight curve is not tangent, it still connects (τ_0, p_0) with (τ_1, p_1) and therefore Eq. (5.69) and Eq. (5.70) still apply. Then between these two points there is an extreme of $S(s)$. Now

$$\begin{aligned}\frac{dS}{d\xi} &= \partial_p S\partial_\xi p + \partial_\tau S\partial_\xi \tau \\ &= (\partial_p S)(\partial_\xi p + \frac{\partial_\tau S}{\partial_p S}\partial_\xi \tau) \\ &= (\partial_p S)(\partial_\xi p + \partial_\tau p\partial_\xi \tau) \\ &= (\partial_p S)(\partial_\xi p + \rho^2 c^2\partial_\xi \tau)\end{aligned} \tag{5.71}$$

Therefore

$$\Big((p_1-p_0)+\rho_0^2c_0^2(\tau_1-\tau_0)\Big)>0 \text{ at } (\tau_0,p_0)\,, \tag{5.72}$$

$$\Big((p_1-p_0)+\rho_1^2c_1^2(\tau_1-\tau_0)\Big)<0 \text{ at } (\tau_1,p_1)\,. \tag{5.73}$$

For $\tau_1>\tau_0$

$$\rho_0^2c_0^2>\frac{p_1-p_0}{\tau_0-\tau_1}>\rho_1^2c_1^2 \tag{5.74}$$

and because dues to conservation of momentum (5.44), from which we have $m^2=\frac{p_1-p_0}{\tau_0-\tau_1}$, we find

$$v_0^2<c_0^2 \quad \text{and} \quad v_1^2>c_1^2\,. \tag{5.75}$$

If we substitute $v_0=u_0-s$ and $v_1=u_1-s$, knowing that the shock speed is larger than the flow speed of either side, we find exactly

$$s<c_0+u_0 \quad \text{and} \quad s>c_1+u_1 \tag{5.76}$$

When we compare these to the Lax entropy conditions, we find that point (τ_0,p_0) is the left side of the wave and (τ_1,p_1) the right side of the wave. Therefore we have $\tau_l<\tau_r$. As the particles cross the shock from right to left, the τ decreases. Since the specific entropy and the density increases as τ decreases, the total entropy increases. Furthermore we also see that the shock is supersonic with respect to the front of the shock and subsonic with respect to the back of the wave. We have thus confirmed that the Lax entropy conditions pick the physically relevant solution which obeys the second law of thermodynamics.

We looked at the jump conditions across the shock to construct the Hugoniot function. By analysing this function we found that between all the left and right states which would be allowed by the jump conditions, the specific entropy would increase if the specific volume would decrease. We then saw that this is equivalent to the results of the Lax entropy conditions. We have therefore now shown that the Lax entropy conditions ensure that entropy increases as the shock wave propagates, exactly as is required by the second law of thermodynamics.

An interesting notion is that for the Euler equations the entropy function and entropy flux, as discussed in Chapter 4, are very intuitive. Consider the new quantity to be the entropy $U=\rho S$, where again S is the specific entropy. We can now use (4.2) to find the derivative of the entropy flux.

$$F'(\mathbf{u})=U'(\mathbf{u})\mathbf{f}'(\mathbf{u})=U'(\mathbf{u})\mathbf{A}(\mathbf{u})\,, \tag{5.77}$$

$$\left(\frac{\partial F}{\partial\rho},\frac{\partial F}{\partial u},\frac{\partial F}{\partial\varepsilon}\right)=\left(\frac{\partial\rho S}{\partial\rho},\frac{\partial\rho S}{\partial u},\frac{\partial\rho S}{\partial\varepsilon}\right)\begin{pmatrix}u & \rho & 0\\ \frac{1}{\rho}\frac{\partial p}{\partial\rho} & u & 0\\ 0 & \frac{p}{\rho} & 0\end{pmatrix}=(S,0,0)\begin{pmatrix}u & \rho & 0\\ \frac{1}{\rho}\frac{\partial p}{\partial\rho} & u & 0\\ 0 & \frac{p}{\rho} & 0\end{pmatrix}=\big(Su,S\rho,0\big)\,. \tag{5.78}$$

This is satisfied for $F=u\rho S$. We can then construct the additional inequality,

$$\frac{\partial}{\partial t}\rho S+\frac{\partial}{\partial x}u\rho S\le 0\,. \tag{5.79}$$

Recall that there is an entropy condition associated with this equation. In this case this is

$$s\left[\rho S\right]\ge[u\rho S]\,, \tag{5.80}$$

$$s\left(\rho_lS_l-\rho_rS_r\right)\ge\left(u_l\rho_lS_l-u_r\rho_rS_r\right)\,, \tag{5.81}$$

$$s\left(\rho_lS_l-\rho_rS_r\right)+\left(u_r\rho_rS_r-u_l\rho_lS_l\right)\ge 0\,, \tag{5.82}$$

$$\rho_rS_r(u_r-s)-\rho_lS_l(u_l-s)\ge 0\,, \tag{5.83}$$

$$\rho_rS_rv_r-\rho_lS_lv_l\ge 0\,, \tag{5.84}$$

By substituting $\rho_r v_r = \rho_l v_l = m$ as the mass flux through the surface of discontinuity, we find

$$mS_r \geq mS_l \,. \tag{5.85}$$

Now going back to our situation, we had particles crossing the shock from right to left. Therefore $m < 0$. This implies $S_l \geq S_r$. And indeed this is exactly what we showed.

Chapter 6

Solving the One-Dimensional Riemann Problem Numerically

In this chapter different methods of solving the Riemann problem will be considered. Computations of fluid dynamics can be quite expensive in terms of computation time and it is therefore interesting to compare different methods. Some numerical methods use solutions or approximate solutions to the Riemann problem to improve the method [8]. Compared to standard discretization methods, this method has the advantages that it is fast and locates shock waves very precise, but the disadvantages are that the found shock waves might violate the entropy conditions and the waves are located inaccurate. We implement these methods in Python to illustrate these advantages and disadvantages in the context of a specific Riemann problem.

6.1 Roe Averaging

The Riemann problem for linear systems of equations has a simple solution. If one were to approximate the Euler equations by a linear system, one could use this simple solution as an approximate solution. We will therefore first discuss the solution to the Riemann problem for linear systems of equations, which is given by

$$\partial_t \mathbf{u} + \mathbf{A}\partial_x \mathbf{u} = \sum_{k=1}^{p} \left(\partial_t \mathbf{l}_k^T \mathbf{u} + \lambda_k \partial_x \mathbf{l}_k^T \mathbf{u} \right) \mathbf{r}_k \,, \tag{6.1}$$

where $\mathbf{u} = \mathbf{u}(x,t)$. Set $\alpha_k = \mathbf{l}_k^T \mathbf{u}$. We then see that

$$\partial_t \alpha_k + \lambda_k \partial_x \alpha_k = 0 \tag{6.2}$$

are scalar equations and have self similar solutions, meaning the solutions depend only on one independent variable instead of both x and t, in this case that is $\frac{x}{t}$. The solutions are given by

$$\alpha(x,t) = \alpha(x - \lambda_k t, 0) = \mathbf{l}_k^T \mathbf{u}_0(x - \lambda_k t) \,. \tag{6.3}$$

We now have the solution

$$\mathbf{u}(x,t) = \sum_{k=1}^{p} \mathbf{l}_k^T \mathbf{u}_0(x - \lambda_k t) \mathbf{r}_k \,. \tag{6.4}$$

Thus given the initial conditions one has to compute the left and right eigenvectors of the Jacobian matrix $\mathbf{A}$ to find the solution. From Equation (6.4) it can easily be seen that the solution consists of three shock waves,

given that the initial conditions contain one jump discontinuity. These shocks are located at $\frac{x}{t} = \lambda_k$, thus the solution is indeed a self similar solution.

The Euler equations are not a linear system. However we can approximate this system with linear approximations. For scalar functions one might use a tangent line approximation or a first order Taylor approximation to approximate the function $f(u)$ near a certain point u_l. Near u_l this is

$$f(u) \approx f(u_l) + f'(u_l)(u - u_l)\,. \tag{6.5}$$

However this approximation is better closer to u_l. Is one wishes to approximate the function over an interval instead of near a point, we can use the secant line approximation. On the interval from u_l to u_r, this is

$$f(u) \approx f(u_l) + a_{RL}(u - u_l)\,, \tag{6.6}$$

or

$$f(u) \approx f(u_r) + a_{RL}(u - u_r)\,, \tag{6.7}$$

where

$$a_{RL} = \frac{f(u_r) - f(u_l)}{u_r - u_l}\,. \tag{6.8}$$

This approximation describes the straight line passing through both u_l and u_r. It is on average better on the whole interval of u_l to u_r. Due to the mean value theorem, $a_{RL} = f'(\xi)$ for some ξ between u_l and u_r. Therefore we can interpret the secant line as an average tangent line on the interval from u_l to u_r.

One can generalise these approximations for scalar functions to approximations for vector functions. The tangent *plane* approximation near $\mathbf{u}_l$ will then be

$$\mathbf{f}(\mathbf{u}) \approx \mathbf{f}(\mathbf{u}_l) + \mathbf{A}(\mathbf{u}_l)(\mathbf{u} - \mathbf{u}_l)\,, \tag{6.9}$$

where $\mathbf{A}(\mathbf{u})$ is the Jacobian matrix of $\mathbf{f}(\mathbf{u})$. The secant plane approximations is

$$\mathbf{f}(\mathbf{u}) \approx \mathbf{f}(\mathbf{u}_l) + \mathbf{A}_{RL}(\mathbf{u} - \mathbf{u}_l)\,, \tag{6.10}$$

where $\mathbf{A}_{RL}$ is a matrix such that

$$\mathbf{A}_{RL}(\mathbf{u}_r - \mathbf{u}_l) = \mathbf{f}(\mathbf{u}_r) - \mathbf{f}(\mathbf{u}_l)\,. \tag{6.11}$$

However there are infinitely many planes passing through both $\mathbf{u}_l$ and $\mathbf{u}_r$. Suppose $\mathbf{f}(\mathbf{u})$ consists of N elements, then $\mathbf{A}_{RL}$ is a matrix with N^2 components. Equation (6.11) is therefore a system of N equations with N^2 unknowns. $\mathbf{A}_{RL}$ is thus not uniquely determined. To determine $\mathbf{A}_{RL}$ we turn back to the scalar case. Here the secant line is an average tangent line on the interval u_l to u_r. Therefore we want the secant plane analogously to be an average tangent plane and thus $\mathbf{A}_{RL}$ is an average of $\mathbf{A}(\mathbf{u})$. We therefore set $\mathbf{A}_{RL} = \mathbf{A}(\mathbf{u}_{RL})$, where $\mathbf{u}_{RL}$ is some average of $\mathbf{u}_l$ and $\mathbf{u}_r$. Now the matrix has only N unknowns. These can be determined by the N equations of (6.11). To motivate this choice of $\mathbf{A}_{RL}$ further, since $\mathbf{A}_{RL} = \mathbf{A}(\mathbf{u}_{RL})$ we can apply all the equations we had for $\mathbf{A}(\mathbf{u})$ to $\mathbf{A}_{RL}$, simply by setting $\mathbf{u} = \mathbf{u}_{RL}$. This makes it possible to use the simple solution from the linear case and directly apply it to this linear approximation. The matrix $\mathbf{A}_{RL}$ is called the Roe-average Jacobian matrix. All quantities derived from this matrix are also referred to as being Roe-averaged.

This method yields three shock waves, while a physical solution of the Euler equations may consist of a shock wave, a contact discontinuity and a expansion fan. In other words, all waves will be replaced by a shock wave, independent of their true nature. As a result the shock which replaces the expansion fan will violate the second law of thermodynamics.

6.2 Forward-Time Central-Space Method

One of the most straightforward ways of numerically solving PDE's in general are finite volume methods. In finite volume methods space and time are discretized. The quantities are then conserved for each cell instead of at each point in space and time. The *ith* cell in space is $[x_{i-1/2}, x_{i+1/2}]$. A quantity $\overline{u}_i^n$ will approximate the cell average of the quantity u in the *ith* cell at time t^n:

$$\overline{u}_i^n \approx \frac{1}{\Delta x} \int_{x_{i-1/2}}^{x_{i+1/2}} u(x, t^n) dx, \tag{6.12}$$

where Δx is the step size of the discretization in the spatial dimension. The the time-averaged the flux through the boundary of the cell during a time step is approximated by $\hat{f}_{i+1/2}^n$.

$$\hat{f}_{i+1/2}^n \approx \frac{1}{\Delta t} \int_{t^n}^{t^{n+1}} f(u(x_{i+1/2}, t)) dt, \tag{6.13}$$

where Δt is the step size of the discretization in the time dimension. The time variation of the conserved quantity in the cell is equal to the flux through the boundary of the cell. This can be represented by the integral form of the conservation law over such a cell during a time step:

$$\int_{x_{i-1/2}}^{x_{i+1/2}} \left(u(x, t^n) - u(x, t^{n+1}) \right) dx = \int_{t^n}^{t^{n+1}} \left(f(u(x_{i-1/2}, t)) - f(u(x_{i+1/2}, t)) \right) dt. \tag{6.14}$$

And will be approximated by the numerical function

$$\Delta x \left(\overline{u}_i^{n+1} - \overline{u}_i^n \right) = -\Delta t \left(\hat{f}_{i+1/2}^n - \hat{f}_{i-1/2}^n \right), \tag{6.15}$$

or equivalently

$$\overline{u}_i^{n+1} = \overline{u}_i^n - \lambda \left(\hat{f}_{i+1/2}^n - \hat{f}_{i-1/2}^n \right), \qquad \lambda = \frac{\Delta t}{\Delta x}. \tag{6.16}$$

We will specifically look at the Forward-Time Central-Space (FTCS) method. Forward-Time implies that the time-averaged flux between t^n and t^{n+1} is approximated by an expression using known values of $\overline{u}$ at times equal or earlier than t^n. The flux at $x_{i+1/2}$ then can be easily approximated by using $f(\overline{u}_i^n)$ and $f(\overline{u}_{i+1}^n)$. Central-Space implies that this is done as following, $\hat{f}_{i+1/2}^n = \frac{f(\overline{u}_i^n) + f(\overline{u}_{i+1}^n)}{2}$. Therefore the FTCS method can be represented by

$$\begin{aligned} \overline{u}_i^{n+1} &= \overline{u}_i^n - \lambda \left(\frac{f(\overline{u}_i^n) + f(\overline{u}_{i+1}^n)}{2} - \frac{f(\overline{u}_{i-1}^n) + f(\overline{u}_i^n)}{2} \right) \\ &= \overline{u}_i^n - \frac{\lambda}{2} \left(f(\overline{u}_{i+1}^n) - f(\overline{u}_{i-1}^n) \right). \end{aligned} \tag{6.17}$$

The computation of $\overline{u}_i^{n+1}$ therefore depends on $\overline{u}_{i-1}^n$, $\overline{u}_i^n$ and $\overline{u}_{i+1}^n$. The direct domain of dependence of $\overline{u}_i^{n+1}$ is therefore $\left(\overline{u}_{i-1}^n, \overline{u}_i^n, \overline{u}_{i+1}^n\right)$. These values in turn also have a direct domain of dependence. The full domain of dependence of $\overline{u}_i^{n+1}$ is the set of all values on which $\overline{u}_i^{n+1}$ depends, including its direct domain of dependence followed by their direct domain of dependence, etc. A point $\overline{u}_i^{n+1}$ also has a physical domain of dependence. This domain is subject to the flow of information in the system. For example the characteristic curves, propagating the initial data, indicate the physical domain of dependence. The physical and numerical domain of dependence must be compared if one wishes that the numerical solution converges to the physical solution. This is done by the Courant-Friedrichs-Lewy (CFL) condition [9]:
A numerical method can be convergent only if its numerical domain of dependence contains the true domain of dependence of the PDE, at least in the limit as Δt and Δx go to zero.

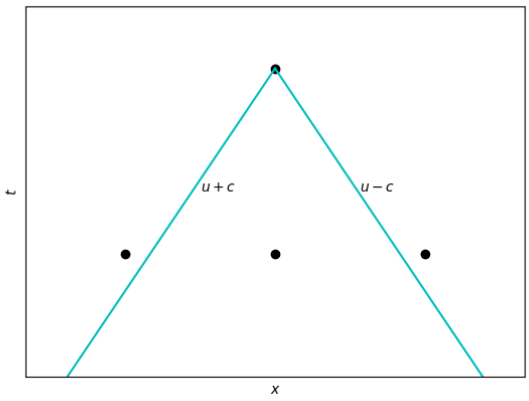

Figure 6.1: *Representation of the boundaries of the physical and numerical domains of dependence. The blue lines indicate the boundaries of the physical domain of dependence. The three lower points indicate the numerical domain of dependence of the upper point. We see that in this figure the physical domain of dependence lies within the numerical domain of dependence.*

The physical domain of dependence for the Euler equations can be expressed in terms of characteristics. The physical domain of dependence of a point in (x,t)-space, is limited by the characteristic with speed $u+c$ from the left and by the characteristic with speed $u-c$ from on the right side of this point. We can see this in Figure 6.1. These lines have slopes $\frac{1}{u+c}$ and $\frac{1}{u-c}$. The numerical domain of dependence is characterised by the lines connecting $\overline{u}_i^{n+1}$ with $\overline{u}_{i-1}^n$ and $\overline{u}_i^{n+1}$ with $\overline{u}_{i+1}^n$. These lines have slopes $\pm\frac{\Delta t}{\Delta x}$. To ensure the physical domain of dependence lies within the numerical domain of dependence, we require

$$-\frac{\Delta t}{\Delta x} \leq \frac{1}{u-c}\,, \tag{6.18}$$

$$u+c \leq \frac{\Delta t}{\Delta x}\,. \tag{6.19}$$

This is always achieved if we choose

$$\frac{\Delta t}{\Delta x} \leq \frac{1}{max\left(|u-c|\,,|u+c|\right)}\,. \tag{6.20}$$

The FTCS method however is proven to be unstable. We will show this following Fourier-Von Neumann analysis. Assume a linear flux. This gives the equation

$$\overline{u}_i^{n+1} = \overline{u}_i^n - \frac{a\lambda}{2}\left(\overline{u}_{i+1}^n - \overline{u}_{i-1}^n\right)\,, \tag{6.21}$$

where $a = \frac{\partial f}{\partial u}$. We make the ansatz that our solution is of the following form

$$u_j^n = \xi^n e^{ikx_j}\,, \tag{6.22}$$

where ξ is complex and k is the spatial wave number. Note that i here denotes the imaginary unit. If $\left|\xi\right| > 1$, then the solution will grow in time. A solution with unbounded growth is an unstable solution. Substituting

this into Equation (6.17) yields

$$\xi^{n+1} e^{ikx_j} = \xi^n e^{ikx_j} - \frac{a\lambda}{2}\left(\xi^n e^{ikx_{j+1}} - \xi^n e^{ikx_{j-1}}\right), \tag{6.23}$$

$$\begin{aligned}\xi &= 1 - \frac{a\lambda}{2}\left(e^{ik(x_{j+1}-x_j)} - e^{ik(x_{j-1}-x_j)}\right)\\ &= 1 - \frac{a\lambda}{2}\left(e^{ik\Delta x} - e^{-ik\Delta x}\right)\\ &= 1 - a\lambda i \sin(k\Delta x).\end{aligned} \tag{6.24}$$

We now conclude $|\xi| = \sqrt{1 + a^2\lambda^2 \sin^2(k\Delta x)} \geq 1$ for all a and k. We can therefore conclude that this method is unstable. A numerical attempt of this method indeed confirmed the instability. For this reason the solution obtained by the FTCS method will not be presented.

6.3 Lax-Friedrichs Method

The Lax-Friedrichs method has a minor modification to the unstable FTCS method,

$$\overline{u}_i^{n+1} = \frac{1}{2}\left(\overline{u}_{i+1}^n + \overline{u}_{i-1}^n\right) - \frac{\lambda}{2}\left(f(\overline{u}_{i+1}^n) - f(\overline{u}_{i-1}^n)\right). \tag{6.25}$$

Applying the same Fourier-Von Neumann analysis yields

$$\xi^{n+1} e^{ikx_j} = \frac{1}{2}\left(\xi^n e^{ikx_{j+1}} + \xi^n e^{ikx_{j-1}}\right) - \frac{a\lambda}{2}\left(\xi^n e^{ikx_{j+1}} - \xi^n e^{ikx_{j-1}}\right), \tag{6.26}$$

$$\begin{aligned}\xi &= \frac{1}{2}\left(e^{ik(x_{j+1}-x_j)} + e^{ik(x_{j-1}-x_j)}\right) - \frac{a\lambda}{2}\left(e^{ik(x_{j+1}-x_j)} - e^{ik(x_{j-1}-x_j)}\right)\\ &= \frac{1}{2}\left(e^{ik\Delta x} + e^{-ik\Delta x}\right) - \frac{a\lambda}{2}\left(e^{ik\Delta x} - e^{-ik\Delta x}\right)\\ &= \cos(k\Delta x) - a\lambda i \sin(k\Delta x),\end{aligned} \tag{6.27}$$

$$|\xi| = \sqrt{\cos^2(k\Delta x) + (a\lambda)^2 \sin^2(k\Delta x)}. \tag{6.28}$$

This does not necessarily lead to an unstable solution. Namely for $a\lambda < 1$ we find $|\xi| < 1$. The modification can be interpreted as numerical diffusion. This modification prevents the instabilities but also causes the solution to be smeared out. Even if $a\lambda < 1$ is satisfied, the solution might still not be stable. Namely the methods also needs to be physically stable.

6.4 Performance

We benchmark these methods with the following problem: Find a solution to the Euler equations at $t = 0.01s$ for the following initial conditions:

$$\begin{array}{ll} p_L = 100000\ \mathrm{N/m^2} & p_R = 10000\ \mathrm{N/m^2} \\ \rho_L = \quad 1\ \mathrm{kg/m^3} & \rho_R = 0.125\ \mathrm{kg/m^3} \\ u_L = \quad 100\ \mathrm{m/s} & u_R = -50\ \mathrm{m/s} \end{array} \tag{6.29}$$

and $\gamma = 1.4$ and $R = 287$ N m/kg K, where p is the pressure, ρ is the density, u is the velocity, γ is the ratio of specific heats and R is the gas constant.

The exact solutions to this problem is given in Figure 6.4. To compare our solutions with this figure, we will calculate the same thermodynamic quantities as used in this figure. Given the initial data, we can calculate the speed of sound c with

$$c^2 = \gamma \frac{p}{\rho}. \tag{6.30}$$

Then the total internal energy can be calculated by

$$e = \frac{u^2}{2} + \frac{1}{\gamma - 1}\frac{p}{\rho}. \tag{6.31}$$

Now we have $(\rho, u\rho, e\rho)^T$, we can apply each of the methods. From the solution we can construct the pressure by

$$p = (\gamma - 1)\left(\rho e - \frac{1}{2}\rho u^2\right). \tag{6.32}$$

Furthermore the entropy can be calculated by

$$s = c_v \ln(p) - c_p ln_{(\rho)}, \tag{6.33}$$

where c_v is the specific heat for constant volume and c_p is the constant pressure specific heat. They are related by $c_p = \gamma c_v$ and $c_p = R + c_v$. The last quantity, the Mach number, is given by the ratio of the velocity over the sound speed

$$M = \frac{u}{c}. \tag{6.34}$$

Then the solutions will be shown by plotting the following quantities: pressure, velocity, speed of sound, density, entropy and Mach number.

The Roe-averaging method calculates three different wave speeds. Between these waves the thermodynamic quantities remain constant as calculated by (6.4). The solution is presented in Figure 6.2. The numerical solution of the Lax-Friedrichs method is presented in Figure 6.3. Furthermore, the solutions at later times have been calculated for the Lax-Friedrichs method. These are plotted to show self-similarity, see Figure 6.6, and the development of the numerical diffusion, see Figure 6.5.

6.5 Discussion on the Computational Methods

We have shown analytically that the FTCS method is unstable and confirmed this with a numerical attempt. Clearly the Roe-averaging method does not capture the expansion fan, while the Lax-Friedrichs method does. However Roe-averaging locates the shock waves very precise, while the Lax-Friedrichs method shows a finite spread of the discontinuities. This is due to the numerical diffusion. To compare these results we will show in Figure 6.4 the exact solutions to the problem, this has been retrieved from Laney [8]. We can see that the Lax-Friedrichs method locates the waves more accurate than the Roe-averaging does. We can therefore conclude that the Lax-Friedrichs method gives a better physical solution in the sense that the different types of waves can be captured and are located correctly. In Figure 6.5 we can see that for the contact discontinuity, the diffusion slightly increases over time and thus the discontinuity gets smoother over time. Furthermore in Figure 6.6 the solution at later times have been scaled so that we can see that the computed solution is indeed self-similar. The Roe-averaging method has a very precise location for each wave without any spread. Moreover the Roe-averaging method is a lot faster than the Lax-Friedrichs method. The time of the Lax-Friedrichs method does however depend on the fineness of the grid. For the solutions with the resolutions as produced in Figures 6.2 and 6.3, the Roe-averaging method was about 2000 times faster. One could try to reduce the number of grid points for the Lax-Friedrichs method. However, this will be at the cost of the resolution of the solution. Similar computation times to that of the Roe-averaging method can be achieved by taking only a handful of grid points, which is for most applications undesired.

We can therefore conclude that the Lax-Friedrichs method gives a more physical accurate solution to the problem, while the Roe-averaging method is significantly faster and locates the shock waves more precise.

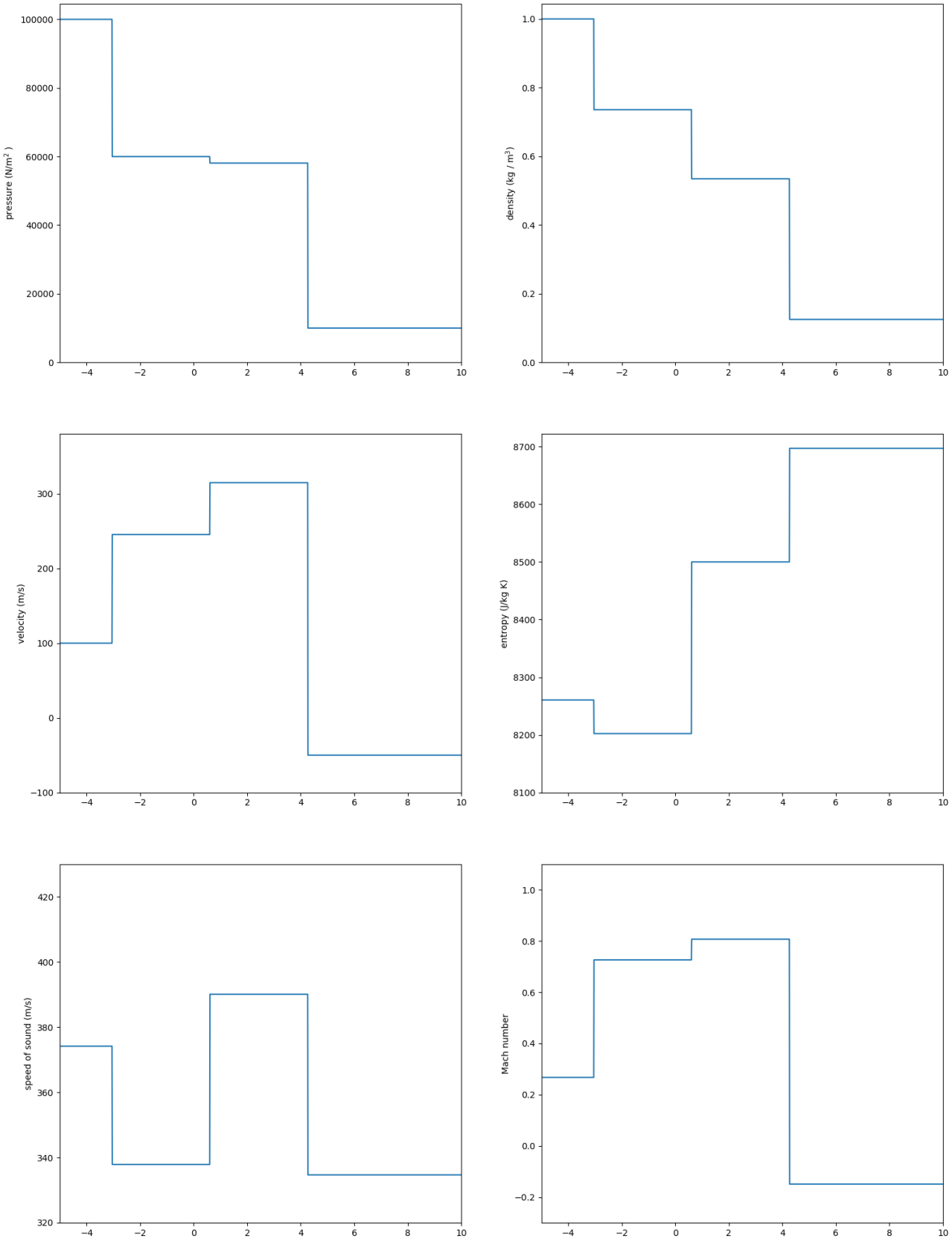

Figure 6.2: *The solution the the posed problem, achieved by Roe-averaging.*

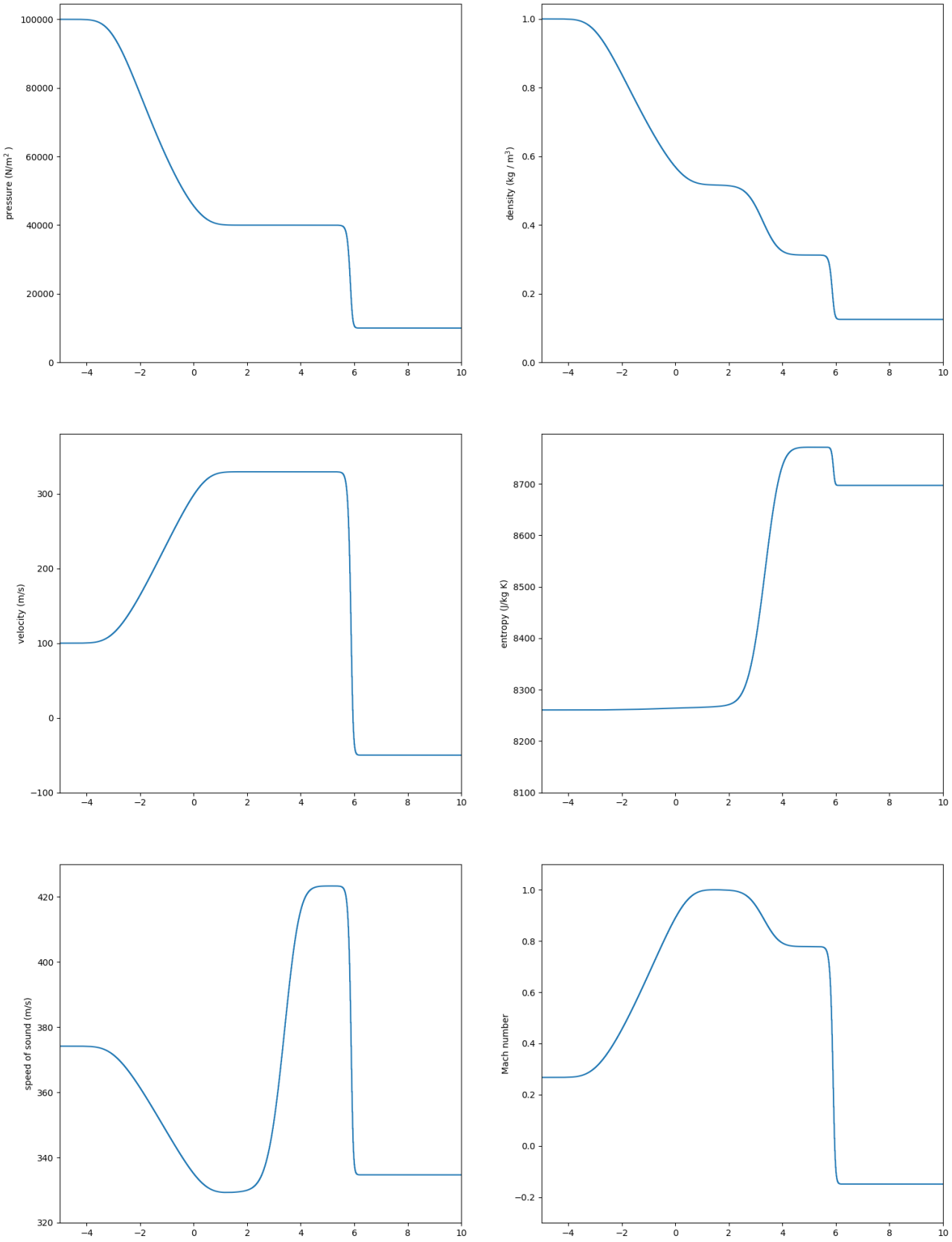

Figure 6.3: *The solution the the posed problem, achieved by the Lax-Friedrichs method.*

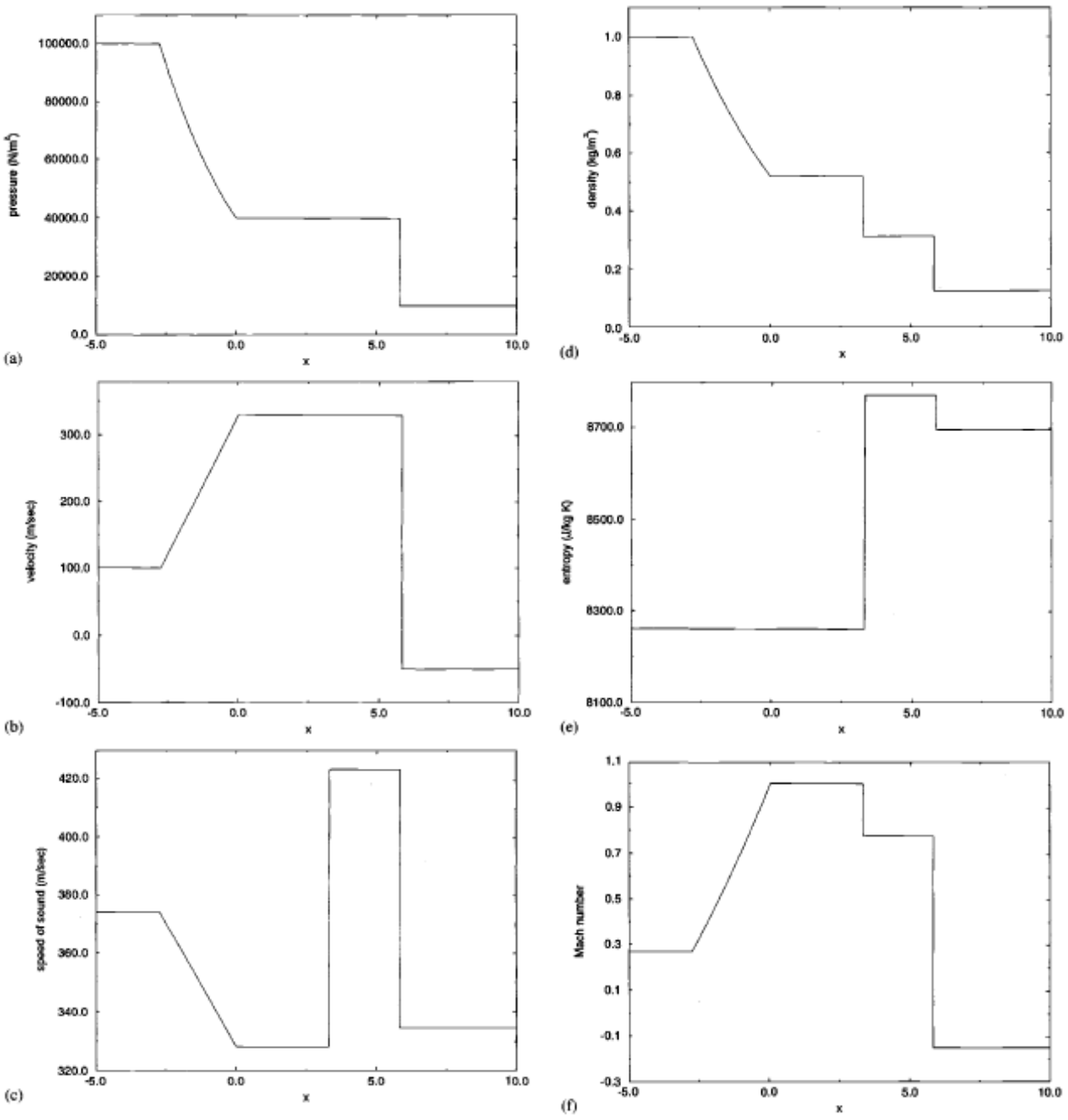

Figure 6.4: *The exact solution to the posed problem. Retrieved from Laney [8].*

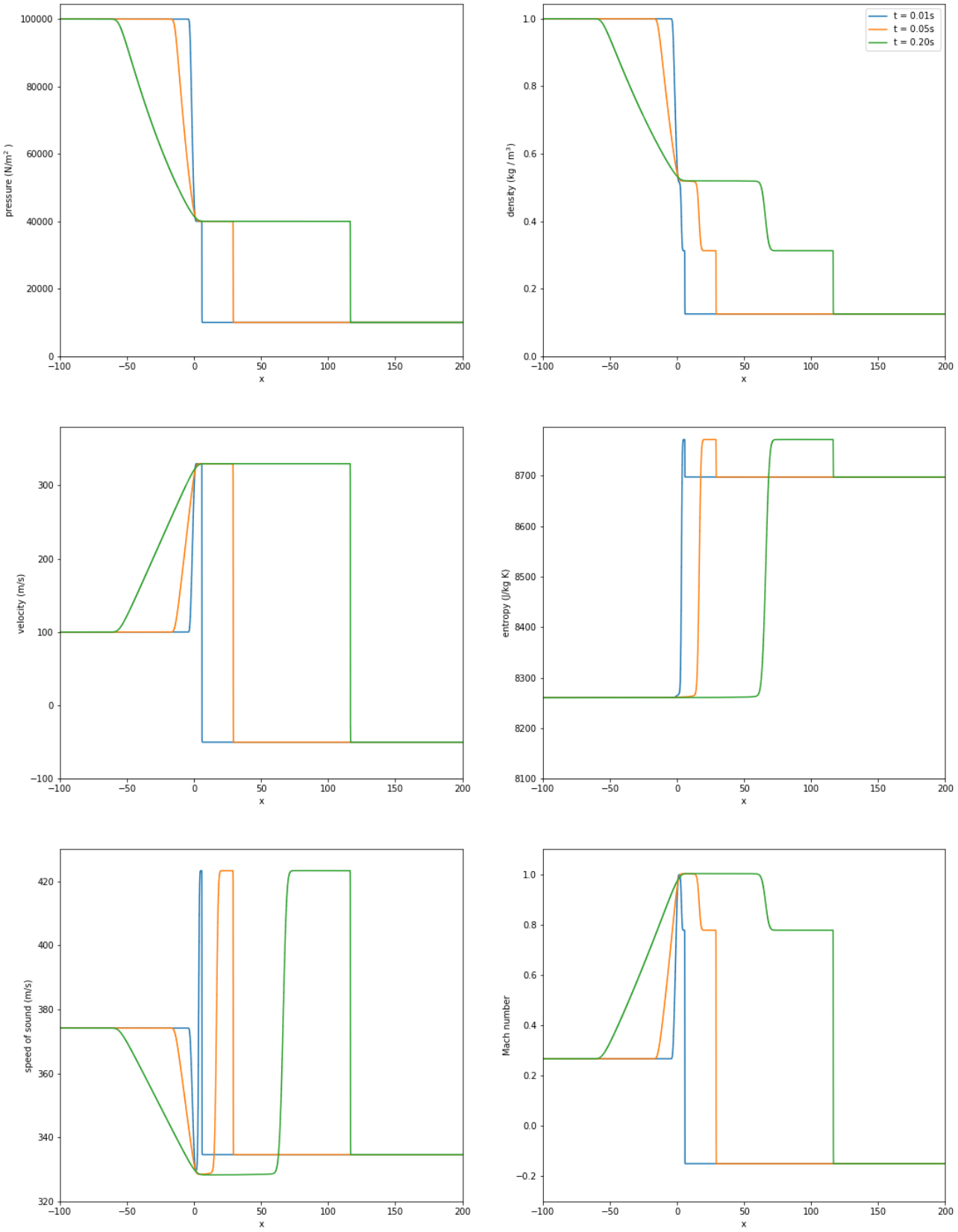

Figure 6.5: *The solution the the posed problem at later moments in time, achieved by the Lax-Friedrichs method. We can see how the waves develop over time.*

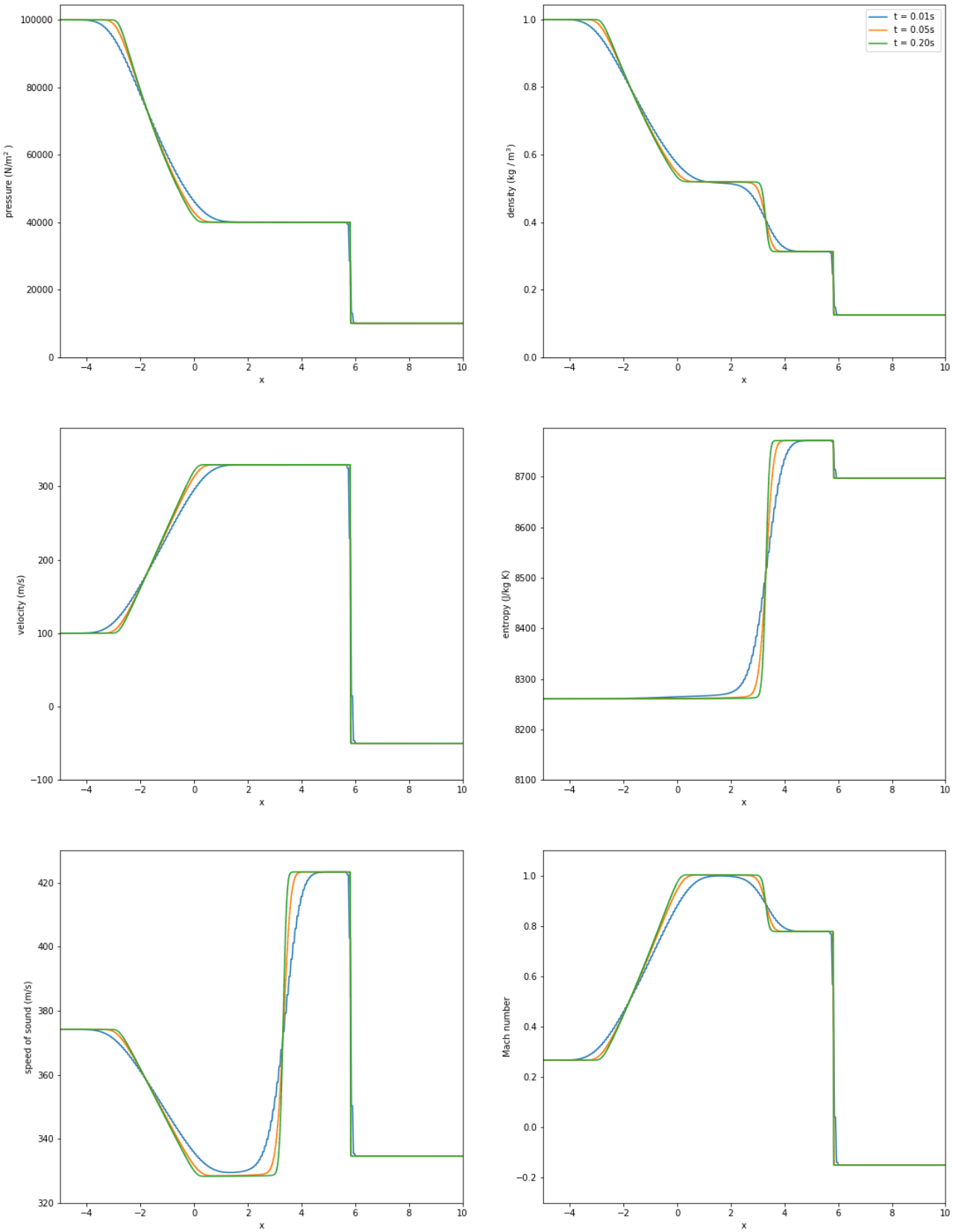

Figure 6.6: *The solution the the posed problem at later moments in time, achieved by the Lax-Friedrichs method. The curves at $t = 0.05s$ and $t = 0.20s$ are scaled to show self-similarity. Their values do therefore not correspond to the x-coordinates.*

Chapter 7

Conclusion

In this thesis we have studied the Riemann problem for hyperbolic conservation laws. We have shown that classical solutions might develop discontinuities after some finite time. To find solutions to the conserved system, while allowing for discontinuities, we turned to the class of weak solutions. These weak solutions are still classical in the domains between the discontinuities. However, at the discontinuities they are not and have to satisfy the Rankine-Hugoniot jump conditions. Furthermore by an example we showed that these mathematical solutions are not unique. To ensure uniqueness and thereby the usefulness to physical problems, entropy solutions were introduced. Specifically for the one dimensional Riemann problem, the conditions to find unique solutions were given by Lax. These conditions ensure that the initial data together with the jump conditions provide enough information to determine a solution for the system uniquely. By applying the Lax entropy conditions to the Euler equations we derived that these equations require particles to cross the shock wave from the front to the back of the wave. That this is equivalent to the increase of entropy was shown by considering the jump conditions across the discontinuity. Therefore this solution will always be consistent with the second law of thermodynamics and we can conclude that these conditions pick the physically relevant solution. The exact solutions of the linear Riemann problem can be used as a foundation for numerical analysis of conservation law problems. We have shown that compared to standard discretization methods, e.g. the Lax-Friedrichs method, this has the advantage that it is a lot faster and locates shock waves very precise. However, this goes at the cost of physical accuracy.

Bibliography

[1] P. D. Lax, *Hyperbolic systems of conservation laws II*, Communications on Pure and Applied Mathematics **10**, 537 (1957).

[2] P. D. Lax, *The Formation and Decay of Shock Waves*, The American Mathematical Monthly **79**, 227 (1972).

[3] E. Godlewski and P.-A. Raviart, *Numerical Approximation of Hyperbolic Systems of Conservation Laws*, Springer, New York, NY, 1996.

[4] *Hyperbolic partial differential equation - Encyclopedia of Mathematics.*

[5] S. N. Kružkov, *First Order Quasilinear Equations in Several Independent Variables*, Mathematics of the USSR-Sbornik **10**, 217 (1970).

[6] R. Courant and K. O. Friedrichs, *Supersonic Flow and Shock Waves*, Springer-Verlag New York, 1976.

[7] H. Weyl, *Shock waves in arbitrary fluids*, Communications on Pure and Applied Mathematics **2**, 103 (1949).

[8] C. B. Laney, *Computational Gasdynamics*, Cambridge University Press, 1998.

[9] R. J. LeVeque, *Finite Volume Methods for Hyperbolic Problems*, Cambridge Texts in Applied Mathematics, Cambridge University Press, 2002.